

How Extreme Apparitions of the Anthropogenic West African Aerosol Plume cause Drought in the Iberian Peninsula, Floods in the U.K. and Ireland and higher winter temperatures in Northern Europe. First Attribution and Mechanism using data from the Terra Satellite, Last Millennium Ensemble, and the MERRA-2 and NCEP/NCAR Reanalyses.

Keith Alan Potts¹

¹Kyna Keju Pty Ltd

November 25, 2022

Abstract

The literature, Inter Governmental Panel on Climate Change (IPCC) and the USA Climate Change Science Program suggest that aerosols can affect the large-scale atmospheric circulation and hydrologic cycle I therefore examine the relationship between aerosols and Iberian droughts, floods in the UK/Ireland and higher European winter temperatures. Aerosols exist mainly as eight continental scale plumes which typically, but not exclusively, exist for a few months in the tropics at the end of the local dry season when biomass burning can occur. The anthropogenic West African aerosol Plume (WAP) exists from late December to early April and is located in the region which drives the northern regional Hadley Circulation towards Europe. It is therefore the prime candidate for investigation into European, winter climate variability. Using the Last Millennium Ensemble (1,156 years and 13,872 months of data) and the MERRA-2 reanalysis (40 years of data) I show that drought in the Iberian Peninsula, floods in the UK/Ireland and higher winter temperatures in northern Europe are created by extreme apparitions of the anthropogenic WAP. The WAP creates these effects by Aerosol Regional Dimming (ARD), which, by altering the surface radiation budget under the plume and warming the upper atmosphere, forces the regional Hadley Circulation into an abnormal seasonal position. These effects alter the regional atmospheric circulation systems and hydrologic cycle in Europe thereby causing drought, floods and higher temperatures and, as the WAP has intensified over recent decades, created climate change.

1 **How Extreme Apparitions of the Anthropogenic West African Aerosol Plume cause**
2 **Drought in the Iberian Peninsula, Floods in the U.K. and Ireland and higher winter**
3 **temperatures in Northern Europe. First Attribution and Mechanism using data from the**
4 **Terra Satellite, Last Millennium Ensemble, and the MERRA-2 and NCEP/NCAR**
5 **Reanalyses.**
6
7

8 **K. A. Potts¹**

9 ¹ Kyna Keju Pty Ltd.

10
11 Corresponding author: Keith Potts (Keith.Potts@bigpond.com)

12 **Key Points:**

- 13 • Winter droughts in the Iberian Peninsula are caused by extreme apparitions of the
14 anthropogenic West African aerosol Plume (WAP).
15 • Simultaneously the WAP also causes winter floods in the U.K. and Ireland and higher winter
16 temperatures in northern Europe.
17 • The WAP creates these effects by perturbing the location of the northern regional Hadley
18 Circulation from late December to early April.
19

20 **Abstract**

21 The literature, Inter Governmental Panel on Climate Change (IPCC) and the USA Climate Change
22 Science Program suggest that aerosols can affect the large-scale atmospheric circulation and
23 hydrologic cycle I therefore examine the relationship between aerosols and Iberian droughts, floods
24 in the UK/Ireland and higher European winter temperatures. Aerosols exist mainly as eight
25 continental scale plumes which typically, but not exclusively, exist for a few months in the tropics at
26 the end of the local dry season when biomass burning can occur. The anthropogenic West African
27 aerosol Plume (WAP) exists from late December to early April and is located in the region which
28 drives the northern regional Hadley Circulation towards Europe. It is therefore the prime candidate
29 for investigation into European, winter climate variability. Using the Last Millennium Ensemble
30 (1,156 years and 13,872 months of data) and the MERRA-2 reanalysis (40 years of data) I show that
31 drought in the Iberian Peninsula, floods in the UK/Ireland and higher winter temperatures in northern
32 Europe are created by extreme apparitions of the anthropogenic WAP. The WAP creates these
33 effects by Aerosol Regional Dimming (ARD), which, by altering the surface radiation budget under
34 the plume and warming the upper atmosphere, forces the regional Hadley Circulation into an
35 abnormal seasonal position. These effects alter the regional atmospheric circulation systems and
36 hydrologic cycle in Europe thereby causing drought, floods and higher temperatures and, as the WAP
37 has intensified over recent decades, created climate change.

38

39 **Plan Language Summary**

40 The West African aerosol plume, one of eight continental scale aerosol plumes
41 (<https://www.essoar.org/doi/10.1002/essoar.10500075.1>), is shown to change the atmospheric
42 circulation systems between West Africa and Europe which creates anomalous, persistent high
43 pressure over the Mediterranean and Iberia. This high pressure forces the winter storms crossing the
44 Atlantic to the north and creates drought in Iberia. The high pressure also creates a persistent south
45 westerly air flow from the central Atlantic into Europe north of the Alps, the UK and Ireland.
46 Coming from further south this air flow is warmer than is usual in this season and this raises the
47 winter temperature in Europe. The airflow is also carrying higher levels of moisture as it originates
48 over warmer seas and, as it reaches the UK and Ireland, it has cooled enough to release this extra
49 moisture as rain resulting in floods in these countries.

50 Hence significant changes in the winter climate in Europe north of the Alps, the UK, Ireland and
51 Spain are caused by the West African aerosol plume and action should be taken immediately to
52 eliminate the plume and which will return the winter climate of Europe to its natural state circa 1950.

1 INTRODUCTION

1.1 HYPOTHESIS AND PHYSICAL MODEL

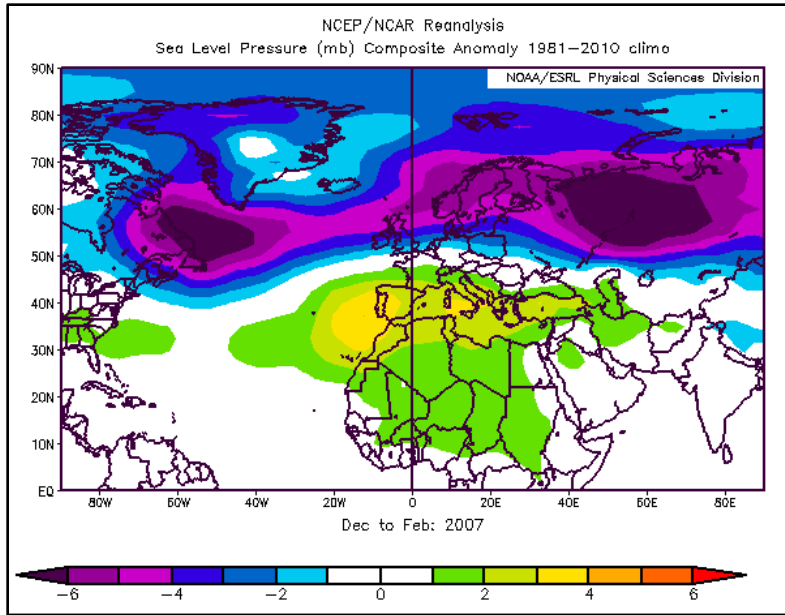
53 *van Oldenborgh et al.* [2009] state that “the observed temperature rise around 52° N is
54 dominated by circulation changes.” and that “a significant increase in air pressure over the
55 Mediterranean (Osborn, 2004) ($z > 3$) and a not statistically significant air pressure decrease over
56 Scandinavia ($z < 2$) have brought more mild maritime air into Europe north of the Alps.”

57 This paper therefore explores an explicit physical model and hypothesis to explain how the
58 West African aerosol Plume (WAP) causes the “significant increase in air pressure over the
59 Mediterranean” which simultaneously creates higher European winter temperatures, drought in the
60 Iberian Peninsula and floods in the UK and Ireland. The sequence of events is:

- 61 1. The anthropogenic aerosol plume forms over West Africa in late December and dissipates
62 in early April with the start of the West African monsoon;
- 63 2. The aerosols absorb (and reflect) solar radiation which heats the atmosphere;
- 64 3. The aerosols reduce the solar radiation at the surface under the plume which cools the
65 surface;
- 66 4. 2 and 3 create a temperature inversion compared to times without a plume and this
67 reduces convection in the region;
- 68 5. The region to the north of the WAP is now the driving force of the convective leg of the
69 northern regional Hadley Cell;
- 70 6. This northerly move in convection perturbs the entire northern Hadley Cell;
- 71 7. This results in higher pressure over the Mediterranean Sea and the Iberian Peninsula;
- 72 8. This forces the cold fronts crossing the Atlantic north and reduces winter rainfall over the
73 Iberian Peninsula;
- 74 9. The high pressure over the Mediterranean Sea and Iberian Peninsula advects warm, moist
75 air from the central Atlantic Ocean into northern Europe
- 76 10. This raises the winter temperature in northern Europe; and
- 77 11. Introduces increased levels of moisture into the U.K. and Ireland and causes floods.

1.2 Pressure over the Mediterranean and the Iberian Peninsula

78 There has been a significant increase in sea-level pressure over the Mediterranean Sea and the
79 Iberian Peninsula in the winter months in recent decades as Figure 1, which recreates part of Figure 7
80 in [*van Oldenborgh et al.*, 2009] from the NCEP/NCAR reanalysis [*Kalnay et al.*, 1996], shows. In
81 Assessment Report 5 (AR5) the IPCC noted: “Changes in atmospheric circulation are important for
82 local climate change because they could lead to greater or smaller changes in climate in a particular
83 region than elsewhere. It is likely that human influence has altered sea level pressure patterns
84 globally.” This is exactly what this paper demonstrates: that the anthropogenic WAP creates the
85 increase in pressure over the Mediterranean and Iberia and it, in turn, drives the changes in the winter
86 climate of Europe.



87
88 Figure 1: NCEP/NCAR Sea-Level Pressure anomaly (Dec to Mar 2007). Note the period of
89 the NCEP climate average is now 1981 to 2010.

1.3 Drought in Spain

90 *García-Herrera et al.* [2007] identified “an impressive northward displacement of cyclone
91 trajectories in the North Atlantic sector in winter months resulting in an almost complete absence of
92 cyclones crossing Iberia and western Europe.” as a significant driver of the 2004/05 hydrological
93 year drought in Iberia and noted that “The results obtained within this work show the [North Atlantic
94 Oscillation] NAO and [East Atlantic] EA indexes, two of the most prominent North Atlantic
95 teleconnection patterns modulating climate in the Iberian Peninsula, incapable to detect the low
96 precipitation totals in March.”

97 *Vicente-Serrano and López-Moreno* [2006] investigated the relationship between the
98 occurrence of drought in NE Spain and atmospheric circulation and found an increase in the number
99 of anti-cyclonic days in winter from 1950 to 2000 which results in lower rainfall in NE Spain. Figure
100 5 in the paper shows Spain covered by higher than average pressure in winter during these days.

101 Trends in sea-level pressure in Europe are shown in *van Oldenborgh et al.* [2009] in Figure 7
102 from 1950–2007 using the NCEP/NCAR reanalysis which show a significant increase in pressure
103 over Iberia and the Mediterranean. Comparisons of observed changes and climate model simulations
104 are also included and the paper states: “In Fig. 7 of the paper trends in sea-level pressure over 1950–
105 2007 of the NCEP/NCAR reanalysis are compared to climate model simulations. Both the reanalysis
106 and the ESSENCE ensemble show a significant trend in the Mediterranean region, but the observed
107 trend is a factor four larger than the modelled trend. The GFDL CM2.1 and MIROC 3.2 T106 models
108 also show significant positive trends in this area, but again much smaller than observed. The other
109 two models show no positive trends there.” Details of the ESSENCE ensemble are provided in [*Sterl*
110 *et al.*, 2008] which shows that in the historic data only tropospheric sulphate aerosols are included
111 and the ESSENCE ensemble cannot therefore have modelled the WAP correctly as it is
112 predominantly composed of carbonaceous aerosols (Appendix A).

113 This paper demonstrates why such an increase in sea-level pressure has occurred over Iberia
114 in winter in recent decades and therefore why the peninsula has endured an increased frequency of
115 drought.

1.4 Floods in the United Kingdom

116 The United Kingdom (UK) has experienced significant floods in winter in recent decades
117 with 2002, 2005, 2009, 2010, 2012, 2014, 2015, 2019 and 2020 noted as significant rainfall/flood
118 events on the UK Met. Office website at [https://www.metoffice.gov.uk/weather/learn-about/past-uk-
119 weather-events](https://www.metoffice.gov.uk/weather/learn-about/past-uk-weather-events) demonstrating a return frequency of just over 2 years. As I write in February 2020
120 storms Ciara and Dennis have just unleashed more UK and Irish floods.

121 In the winter of 2013-14 a rapid succession of Atlantic low pressure systems crossed the UK
122 with large increases in rainfall in the south of England and much of Scotland [Huntingford et al.,
123 2014] who noted “The role of anthropogenic aerosol effects requires further work, especially on
124 tropical atmospheric circulation and hence rainfall, given high regional variations in concentration of
125 aerosols compared with well-mixed GHGs”. This is the focus of this paper.

126 Schaller et al. [2016] also investigated the 2014-15 floods using a regional climate model
127 covering the UK and eastern North Atlantic Ocean to investigate the effects of anthropogenic
128 emissions on the winter climate of the UK. However, the only mention of aerosols in the paper refers
129 to “sulphate aerosol precursors” and it cannot therefore have included the carbonaceous aerosols
130 which constitute the WAP which this paper addresses. They did note “More studies of this nature are
131 needed if loss and damage from anthropogenic climate change are to be quantified objectively and
132 future assessments of the impacts of climate change are to progress from attributing them simply to
133 changes in climate which are not themselves explained, to attributing them specifically to human
134 influence.” Which, again, is exactly what this paper does.

1.5 Higher Winter Temperatures in Northern Europe

135 The IPCC has identified Europe as one of the fastest warming regions of the world and in
136 Assessment Report 4 (AR4) discussing changes since 1979 stated: “Warming in this period was
137 strongest over western North America, northern Europe and China in winter”. IPCC AR5 states
138 “Regardless of whether the statistics of flow regimes themselves have changed, observed
139 temperatures in recent years in Europe are distinctly warmer than would be expected for analogous
140 atmospheric flow regimes in the past, affecting both warm and cold extremes citing [Yiou et al.,
141 2007] and [Cattiaux et al., 2010]”

142 The European winter of 2006-07 was exceptionally warm and the New Scientist reported that
143 “the temperatures experienced during autumn 2006 and winter 2007 are likely to have been the
144 warmest in 500 years, they say. But the sequential combination of two such warm seasons is a still
145 rarer event - probably the first since 1289” citing *Luterbacher et al.* [2007]. *van Oldenborgh et al.*
146 [2009], based on *Osborn* [2004], states the winter temperature rise in Europe is dominated by
147 circulation changes that bring mild maritime air into Europe north of the Alps and, as noted above,
148 climate modelling fails to replicate these circulation changes – specifically the higher pressure over
149 the Mediterranean Sea and Iberia.

150 *Osborn* [2004] used an ensemble of seven climate models and observations to analyse the
 151 significance of the trend noting: “An improved understanding of past precipitation would help
 152 towards improved regional-scale projections of the future, which are of huge value to policymakers.”

153 Figure 1 from the NCEP/NCAR reanalysis dataset shows the high-pressure anomaly
 154 discussed by [*van Oldenborgh et al.*, 2009]. Such an area of persistent high-pressure over the
 155 Mediterranean Sea advects warm air from the central Atlantic to northern Europe resulting in
 156 anomalously high temperatures as noted by *van Oldenborgh et al.* [2009]

157 These cited papers suggest that the climate modelling which was reviewed does not include
 158 the forcing agent which caused the rise in pressure over the Mediterranean and Iberia which this
 159 paper shows to be the carbonaceous, anthropogenic WAP.

1.6 Aerosols and Climate

160 The IPCC Assessment Report 4 (AR4) [*Solomon et al.*, 2007] identifies the two main
 161 anthropogenic contributors to climate change as Long Lived Green House Gases (LLGHG) and
 162 aerosols and defines Radiative Forcing (RF) as the global annual average of “the change in the net,
 163 downward minus upward, irradiance (expressed in W m^{-2}) at the tropopause”. The IPCC AR4 also
 164 discusses Surface Forcing (SF), the effects of the forcing agents at the surface of the Earth and Figure
 165 2 from that report shows the evolution of RF and SF from 1850 to the present day. It can be clearly
 166 seen that the net anthropogenic RF effect, black line – panel (A), follows the red line of LLGHG
 167 reasonably closely. However, the net anthropogenic SF effect, black line – panel (B), clearly follows
 168 the evolution of the aerosol direct effect which is much larger than the aerosol direct RF effect. The
 169 SF graph also shows that the anthropogenic, globally and annually averaged aerosol direct effect in
 170 2000 at -1.6W/m^2 is comparable to the explosive volcanic eruptions of Krakatau (1883) -2.2W/m^2
 171 and Pinatubo (1991) -1.8W/m^2 which are considered to affect the mid to high latitude atmospheric
 172 circulation patterns [*Solomon et al.*, 2007].

173 Absorbing aerosols, particularly black carbon, a product of incomplete combustion [*Novakov*
 174 *et al.*, 2003], and organic carbon [*Kirchstetter*, 2004], have been linked to variations in the vertical
 175 temperature profile of the atmosphere and the large scale atmospheric circulation [*Solomon et al.*,
 176 2007], [*Menon et al.*, 2002] and [*Wang*, 2004]. Aerosols may also have a greater influence on the
 177 hydrologic cycle than other forcing agents through their SF effects [*Solomon et al.*, 2007].

178 *Knippertz et al.* [2015] discuss the effects of aerosols on the West African monsoon noting
 179 that “In West Africa, biomass burning is a large direct source of carbonaceous aerosols” and
 180 “Biomass burning occurs predominantly during the dry season. It is almost exclusively
 181 anthropogenic...”. It is also noted that “more attention should be paid to rapidly increasing air
 182 pollution over the explosively growing cities of West Africa, as experiences from other regions
 183 suggest that this can alter regional climate through the influences of aerosols on clouds and
 184 radiation”.

185 *Solomon et al.* [2007] expressed the concern that the distribution and evolution of aerosol
 186 emissions during the 20th century were not well understood and *Hegerl et al.* [2007] noted that most
 187 studies used in the IPCC AR4 omitted carbonaceous aerosols which could have significant effects at
 188 regional scales.

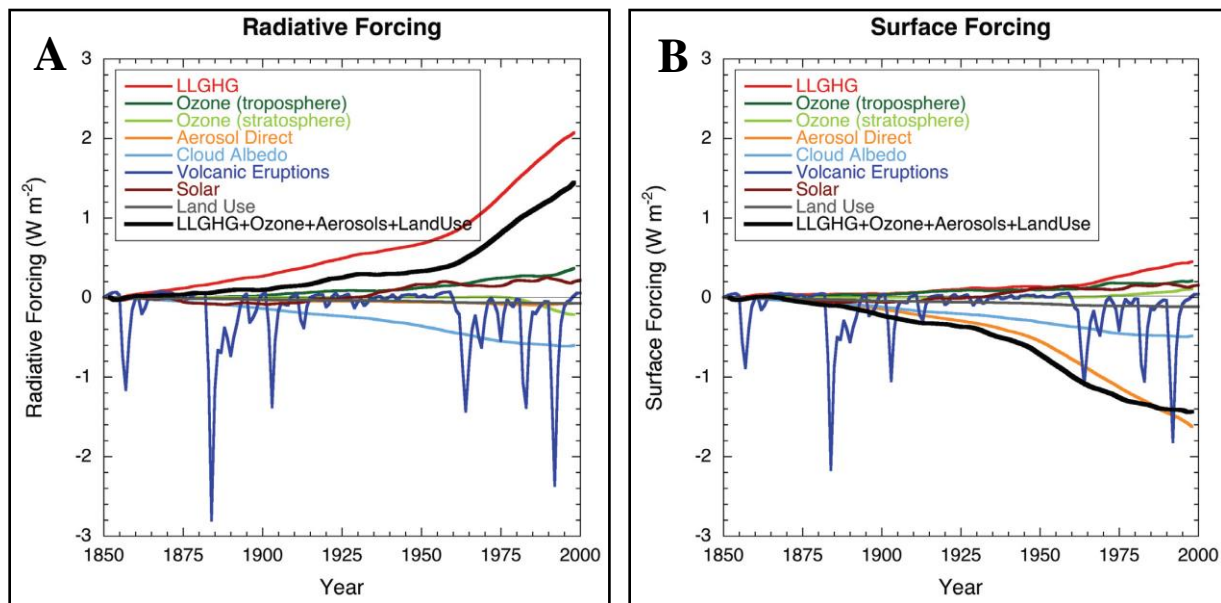
189 The effects of short lived gases and aerosols were found to be substantial compared to
 190 LLGHG and to account for as much as 40% of the warming over the summertime United States and

191 the climate response to these forcing agents was not confined to the area of their emission [Levy II et
192 al., 2008].

193 The global aerosol coverage and forcing is highly variable geographically and temporally and
194 it is “insufficient or even misleading” to emphasise the global average and the aerosol SF is greater
195 than the RF at the top of the atmosphere. Such SF affects the atmospheric circulation and the
196 hydrologic cycle [Remer et al., 2009].

197 *Menon et al.* [2002] investigating the climate of China and India found precipitation and
198 temperature changes in their model that were comparable to those observed only if the aerosol
199 ensemble included a large proportion of absorbing black carbon (“soot”) which was similar to
200 observed amounts and noted that absorbing aerosols heat the atmosphere and alter the regional
201 atmospheric stability and vertical motions which affects the large-scale circulation and hydrologic
202 cycle with significant regional climate effects.

203



204
205 Figure 2: IPCC AR4 Figure 2.23 Chapter 2 page 208 [Forster et al., 2007]. Globally and
206 annually averaged temporal evolution of the instantaneous all-sky RF (A) and SF (B) due to various
207 agents, as simulated in the MIROC+SPRINTARS model (Nozawa et al., 2005; Takemura et al.,
208 2005). This is an illustrative example of the forcings as implemented and computed in one of the
209 climate models participating in the AR4. Note that there could be differences in the RFs among
210 models. Most models simulate roughly similar evolution of the LLGHGs’ RF.

211 Anthropogenic aerosols have been linked to: the decadal variance in the North Atlantic SST
212 and thus to drought in the Sahel and the Amazon with the dominant mechanism being the reduction
213 in short wave surface radiation [Booth et al., 2012]; and the expansion of the tropics in the northern
214 hemisphere evidenced by a poleward shift of the Hadley Cells, subtropical dry zones and extra-
215 tropical storm tracks [Allen et al., 2012] who identify West Africa as one of the regions of the globe
216 which has demonstrated increases in black carbon emissions of $1ng/Kg$ from 1970 to 2009. However
217 *Zhang et al.* [2013] investigated the claims in [Booth et al., 2012] and concluded that “key aspects of
218 the HadGEM2-ES simulation exhibit substantial discrepancies with observations.” Whilst noting that

219 “Anthropogenic and natural aerosols have likely played some role in forcing the observed Atlantic
220 multidecadal variability.”

221 [Ott *et al.*, 2010] investigated the extreme biomass burning episode in the south East Asia in
222 2006 and found that “temperatures over Indonesia were strongly modified by increased diabatic
223 heating during the period of burning. The largest increases were found in October and November
224 between 150 and 400 hPa. In some regions, increases exceeded 0.7 K during SON.” and that it is
225 necessary for GCMs to include realistic representations of aerosols which fully represent the
226 interannual variability of biomass burning emissions in order to capture the effects discussed in their
227 paper.

228 The carbonaceous aerosol emission inventories for the Coupled Model Intercomparison
229 Project phase 5 (CMIP5) are based on *Lamarque et al.* [2010] and are decadal averages designed to
230 investigate long term (decadal to century) climate change and *Lamarque et al.* [2010] specifically
231 state the emission inventories for CMIP5 are not designed to investigate “rapid” (i.e. less than a few
232 years) pollution changes which this paper addresses.

233 *Booth et al.* [2012] also note that future emissions of anthropogenic aerosols are “directly
234 addressable by policy actions”.

235 In summary then the literature states aerosols affect:

- 236 1. The hydrologic cycle;
- 237 2. The large-scale atmospheric circulation systems; and
- 238 3. are not well understood;

239 and that carbonaceous aerosols:

- 240 1. Are an essential parameter in climate models to correctly model observed changes in
241 precipitation;
- 242 2. Were omitted from most studies used in the IPCC AR4;
- 243 3. Have recently been linked to significant climate events; and
- 244 4. Are only included in the CMIP 5 RCP’s as decadal averages which cannot model the effects
245 this paper addresses.

246 and that aerosol emissions are directly addressable by government policy actions.

247 The term Aerosol Regional Dimming (ARD) describes the surface radiative forcing effect of
248 continental scale aerosol plumes which immediately alters the large-scale atmospheric circulation
249 systems and regional hydrologic cycle and, crucially, only occurs when the plume exists.

1.7 The Anthropogenic West African Aerosol Plume

250 The major anthropogenic aerosol plume located in the region most likely to affect the
251 European region Hadley Circulation occurs over West Africa and is referred to as the West African
252 aerosol Plume (WAP).

253 The WAP is one of eight great aerosol plumes [*Potts*, 2017] which occur annually. It can be
254 identified on the monthly mean 0.55 micron AOD data from MODIS [*Kaufman et al.*, 2000] on the
255 NASA Terra and Aqua satellites distributed via the NASA MODIS Giovanni System (NMGS).

256 *Remer et al.* [2005] confirm that the uncertainty in the AOD measured by these two satellites is
 257 “ $\Delta\tau=\pm 0.05 \pm 0.15\tau$ over land” and that the AOD retrievals can be used in monitoring the aerosol
 258 radiative forcing of the global climate. The area used to analyse the WAP is 0° to 10°N 0° to 10°E
 259 (WAP Area).

260 The monthly average AOD of the WAP Area and the annual AOD cycle are shown in Figures
 261 3 and 4 to demonstrate the peak anthropogenic aerosol emission season is January, February and
 262 March (JFM), the end of the dry season in West Africa, and was extremely high in 2004, 2007, 2012,
 263 and 2016 compared with the intervening years. This paper therefore focuses on the anthropogenic
 264 WAP in JFM because it is at its most intense in this season and will therefore have its greatest effect
 265 at this time. Figure 4 shows the trend in AOD since 1980 using the MERRA-2 reanalysis data and
 266 Figure 5 shows the geographic extent of the JFM 2004 extreme apparition of the WAP and clearly
 267 shows the origin of the plume to be in southern Nigeria as the highest AOD levels are seen there.

268 The maximum AOD for the WAP Area measured by the MODIS sensor on the Terra
 269 platform was 1.32 (Mar 2004) and the trend line of the MERRA-2 AOD in JFM in the WAP Area
 270 increased from 0.5 in 1980 to 0.76 in 2019 a 52% increase. From 1980 to 2004, a major biomass
 271 burning event year, the increase in AOD in March was from 0.37 to 1.10 an increase of 197%.

272 *Oluleye et al.* [2012] investigated the relationship between the AOD retrievals from the
 273 NASA Terra and Aqua satellites and ground-based photometers in West Africa and found good
 274 correlations, over 0.90, at Ilorin in Nigeria. Figure 2 in that reports clearly shows the seasonal
 275 variation in the AOD levels with many days showing AOD levels at Ilorin over 1.00 in JFM from
 276 2005 to 2009.

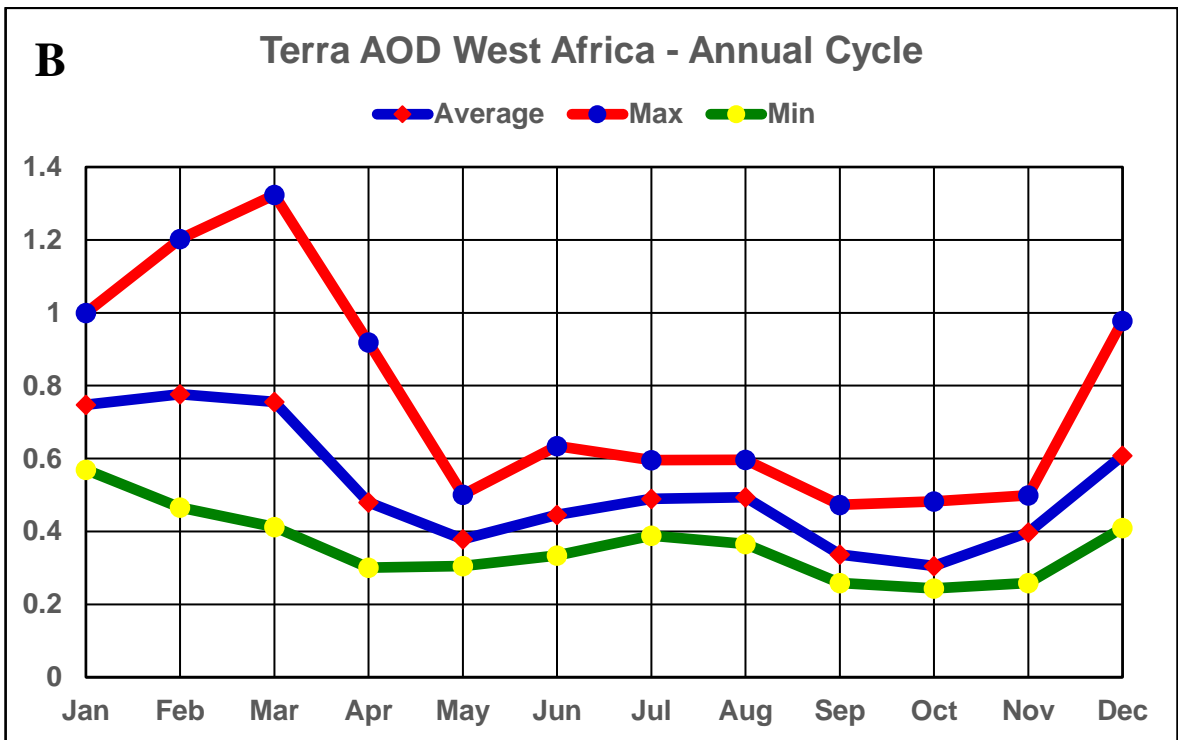
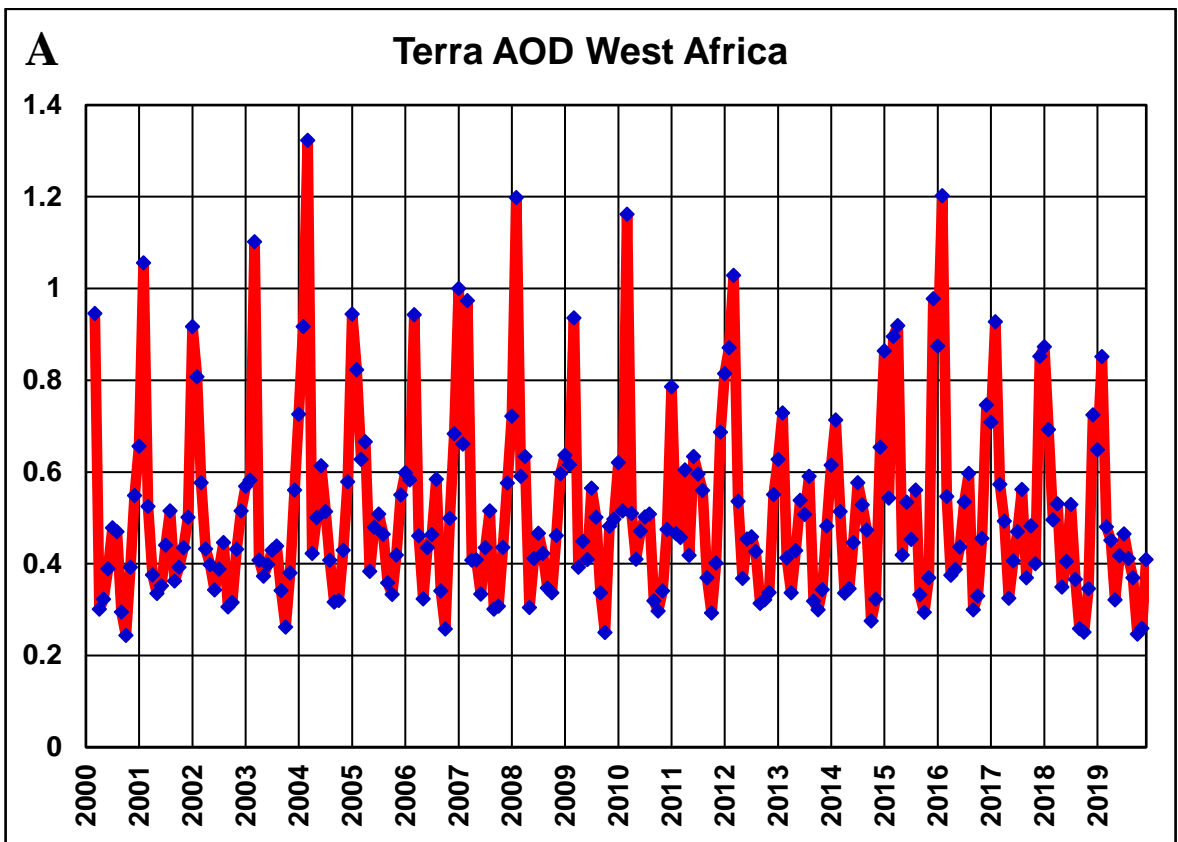
277 **WAP History:** Figure 4 shows a significant trend in the AOD of the WAP from 1980 to 2019
 278 and the WAP AOD would have been significantly lower in 1950 than it was in 1980 for two reasons:

- 279 • First: the population of West Africa was significantly higher in 1980 (188 million) c.f. 1950
 280 (71 million) (United Nations World population data for West Africa) which implies less
 281 biomass burning from agriculture and land clearing; and
- 282 • Second: oil production had not started in Nigeria in 1950 (Nigerian National Petroleum
 283 Corporation in “History of the Nigerian Petroleum Industry” at
 284 [https://www.nnpcgroup.com/NNPC-Business/Business-Information/Pages/Industry-](https://www.nnpcgroup.com/NNPC-Business/Business-Information/Pages/Industry-History.aspx)
 285 [History.aspx](https://www.nnpcgroup.com/NNPC-Business/Business-Information/Pages/Industry-History.aspx) and there were therefore no gas flares driven by oil production in Nigeria in
 286 1950.

287 This suggests that the AOD of the WAP in JFM in 1950 would have been beneath 0.19 on the
 288 basis of pro rata population growth alone and perhaps beneath 0.1 without the gas flares. This implies
 289 the effects of the extreme WAP are very recent and that the anthropogenic WAP did not exist in its
 290 present extreme state in JFM prior to or in the early 1950’s.

291 The main sources of aerosols in the WAP are described in detail in Appendix A.

292

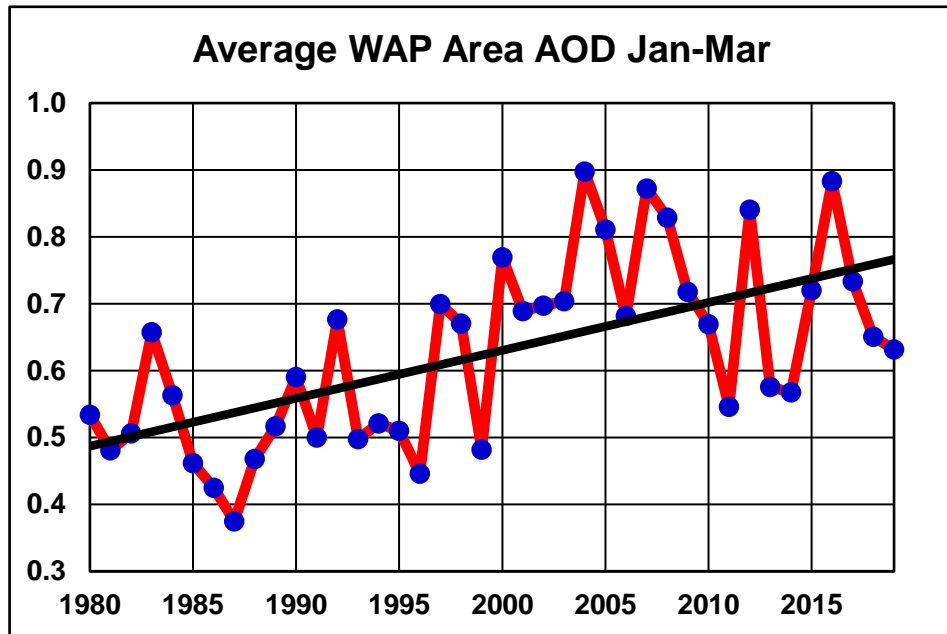


294

295

Figure 3: Terra Monthly AOD WAP Area. A; Average, Max and Min Annual cycle B.

296

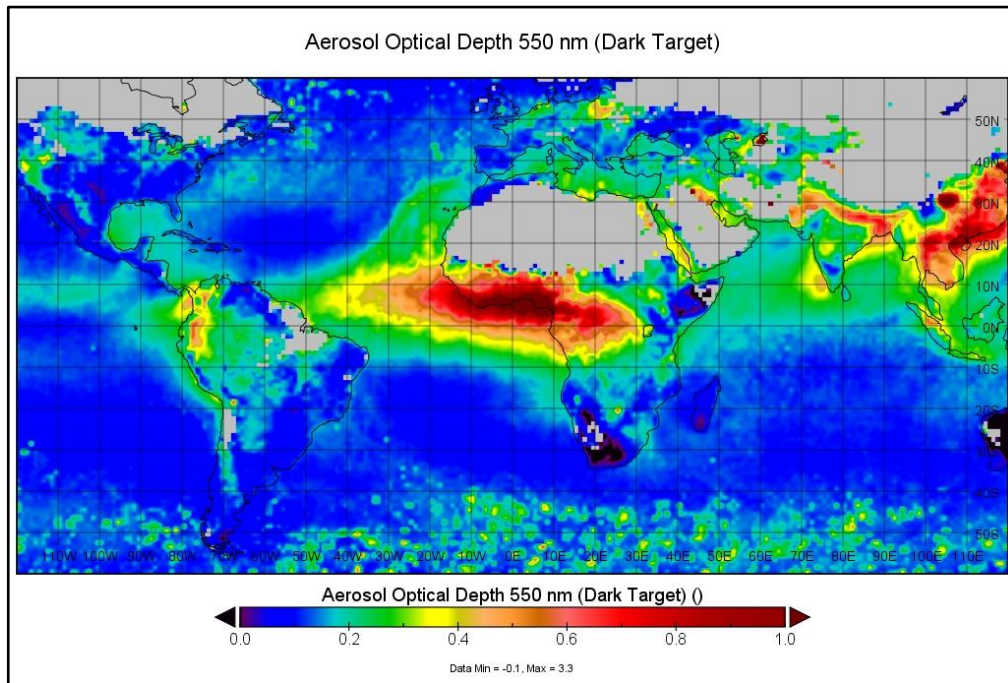


297

298

Figure 4: Average MERRA-2 JFM AOD WAP Area.

299



300

301

302

Figure 5: NASA Terra average AOD Jan - March 2004.

303

1.8 Surface Radiative Forcing by Aerosols

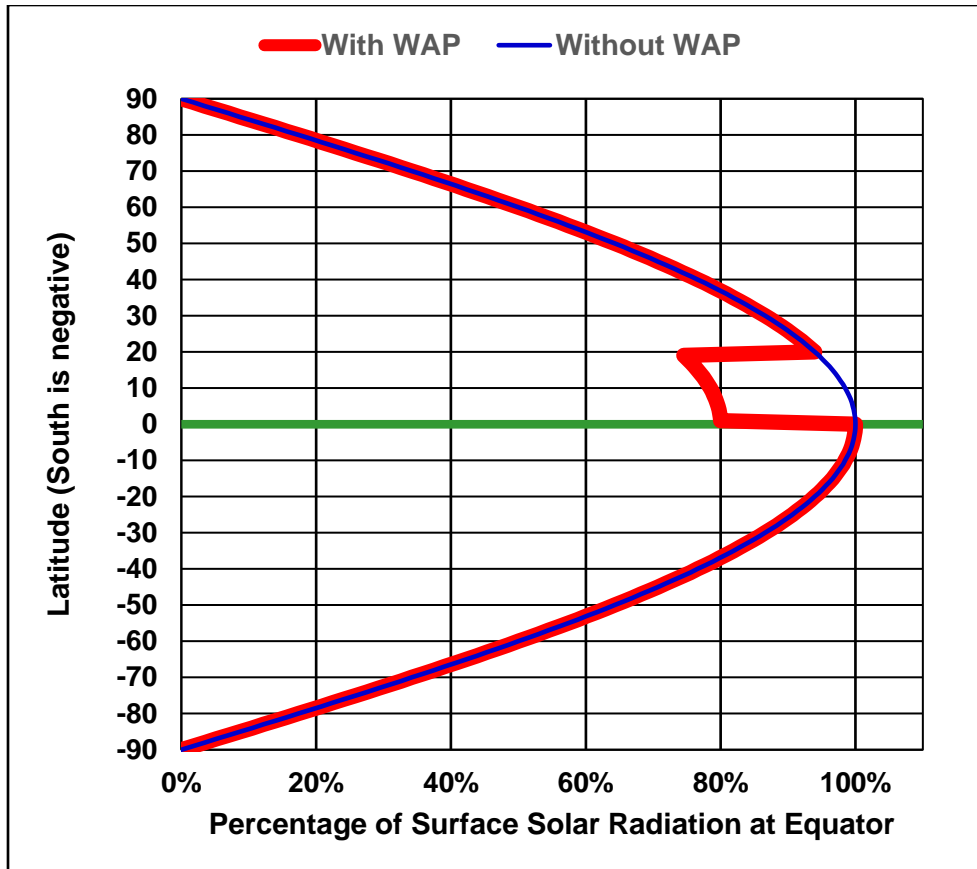
304 The SF of aerosols is significant and the literature includes:

- 305 1. a 10% to 30% reduction of Photosynthetically Active Radiation recorded during
306 INDOEX in the Indian Ocean in 1999 [Ramanathan, 2006];
- 307 2. -150 W m^{-2} in an analysis of the Indonesian wildfires which occurred in 1997 in
308 [Duncan et al., 2003]; and
- 309 3. $\sim -286.0(\text{W/ m}^2)/\tau\alpha$ recorded during the Aerosol Characterization Experiment -Asia in
310 2001 [Hansell et al., 2003] ($\tau\alpha$ is the aerosol optical depth and its derivation is described
311 in the paper).

312 The idealised change in direct surface radiation when the WAP is present is shown in Figure
313 6 with a plume AOD estimated at 0.8 compared with background 0.58 giving an estimated 20%
314 reduction in surface radiation noting that 0.8 is less than the maxima shown in the MERRA-2 data in
315 Figure 4 and 0.58 is greater than lower minima in the same Figure which implies the actual reduction
316 in surface radiation may be greater than 20%. In Figure 6 the sun is assumed to be over the equator
317 and the phase lag between the sun and the position of the ITCZ is ignored. It is clear that the highest
318 level of surface solar radiation is at the edges of the plume and that these regions will drive
319 convection which, in turn, drive the Hadley Cells. With the convective drive of the regional northern
320 Hadley Cell moving north the entire northern regional Hadley Cell is perturbed which in turn
321 perturbs the regional sub-tropical ridge in the northern hemisphere and creates anomalous, persistent,
322 high pressure over the Mediterranean, Iberia and the Eastern Atlantic (MIEA) as a direct
323 consequence of the WAP.

324

325



326

327 Figure 6: Idealised surface solar radiation with and without the WAP assuming a reduction
 328 surface radiation of 20% and a 20° latitude width of the WAP from 0° to 20°N.

2 METHOD and DATA

2.1 Modelling Data

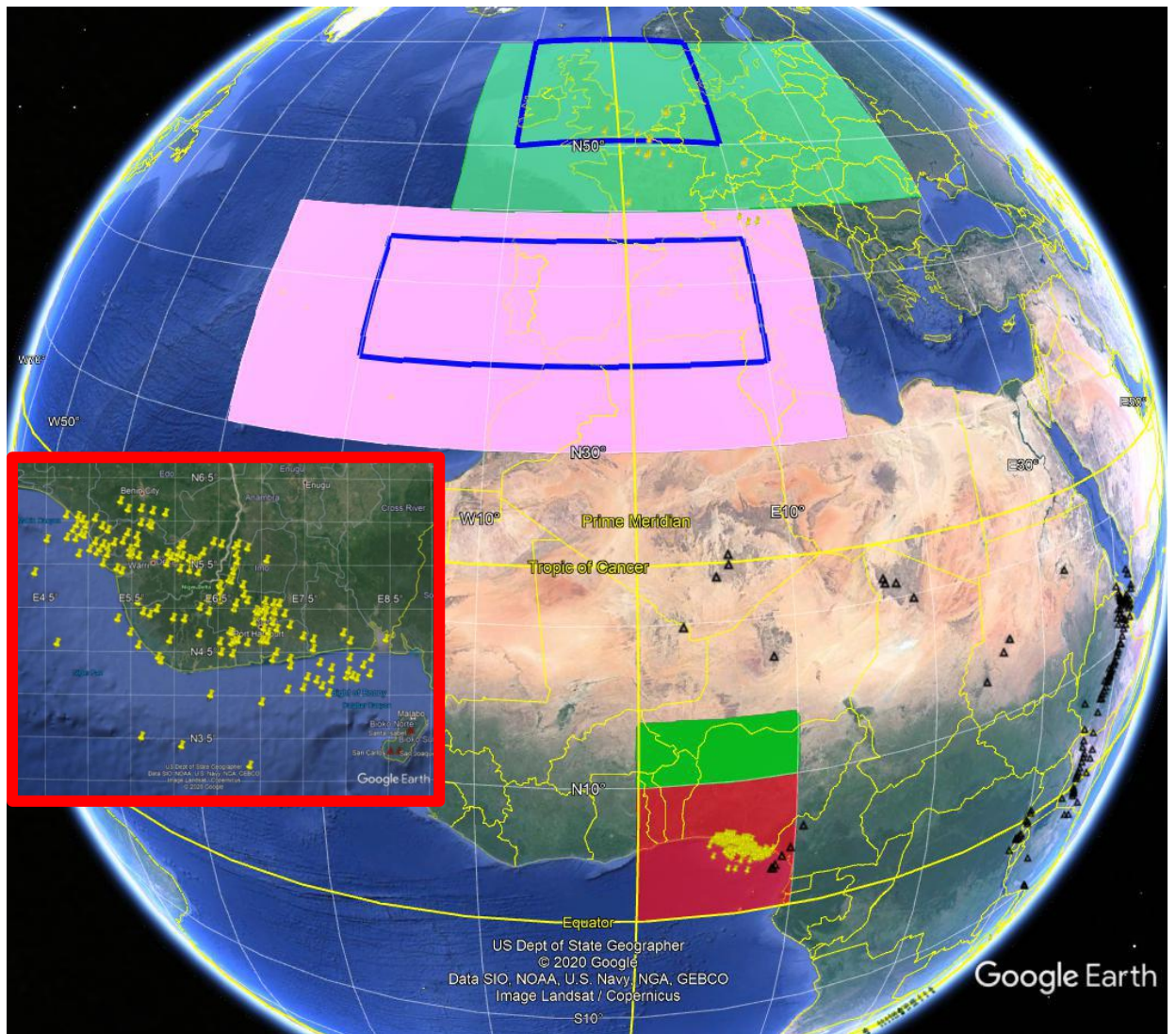
329 The Last Millennium Ensemble (LME) [Otto-Bliesner *et al.*, 2016] data is available at
 330 <https://www.earthsystemgrid.org/>. One member of each of the eight LME forcing simulations with
 331 run number in () (850 (3), All (13), Ozone and Aerosol (Aero) (2), Green House Gas (GHG) (3),
 332 Land use (Land) (3), Orbital (3), Solar (5) and Volcanic (5)) was used to create time series of 1,156
 333 years of: AODVIS (hereinafter AOD); surface pressure (PSL), surface temperature (TS);
 334 precipitation (PRECL) and vertical pressure velocity (hereinafter “omega”); The LME data was
 335 averaged to give annual and JFM time series from 850 to 2005 and then correlated with the WAP
 336 AOD as a time series to demonstrate that these indices and parameters are directly connected to
 337 aerosols in the WAP area.

338 The data was also segmented and averaged on the basis of AOD and then correlated and is
 339 also presented graphically to show the effects of changes in AOD without using correlation.

340 Areas used for the LME data (Descriptors in ()) are shown in Figure 7 and are:

- 341 • AOD (WAP Area): 0° 10°N and 0° 10°E

- 342 • Surface Temperature (WAP Area) 0° 10'N and 0° 10'E
- 343 • Omega West Africa (W. Africa) 10° 15'N and 0° 10'E
- 344 • Pressure (Mediterranean, Iberia, Eastern Atlantic (MIEA)): 30° 45'N and 30°W 15'E
- 345 • Rainfall Southern Europe (Iberia): 35° 43'N and 20°W 10'E
- 346 • Rainfall Northern Europe (UK/Ireland): 50° 60'N and 10°W 10'E
- 347 • Temperature (N. Europe): 45° 60'N and 15°W 30'E
- 348



349 Figure 7: Google Earth image showing areas used and the locations of Nigerian gas flares
 350 (National Oceanic and Atmospheric Administration (NOAA) and the Global Gas Flaring Reduction
 351 Partnership (GGFRP)) in yellow and African volcanoes (Global Volcanism Program) in black. Inset
 352 southern Nigerian gas flares.

2.2 MERRA-2 Data

353 A similar approach was used for the NASA Modern Era Retrospective analysis for Research
354 and Applications release two (MERRA-2) reanalysis dataset [Gelaro *et al.*, 2017] which is an
355 atmospheric reanalysis of the modern satellite era produced by NASA's Global Modelling and
356 Assimilation Office. MERRA-2 is especially useful for the analysis in this paper as it includes the
357 assimilation of aerosol observations and extended for 40 years in 2019. The aerosol loading in the
358 WAP area is variable with significant spikes at near random intervals making it especially useful in
359 correlation analysis. Data <http://giovanni.gsfc.nasa.gov/giovanni/>

3 RESULTS

360 The climate is highly variable with more than one agent usually contributing to any variation
361 and therefore whilst useful information can be extracted from such data using only time series
362 analysis it is preferable to also analyse the data by segmenting the data on the basis of the forcing
363 agent being investigated, averaging and then correlating as the averaging process improves the signal
364 to noise ratio in the data significantly and the range of the forced parameter from the lowest to the
365 highest forcing segment shows the effects of the forcing agent without relying on correlation.

366 The LME time series correlations are presented in Figure 8 where the time series annual data
367 shows lower correlation magnitudes than the JFM data. This results from the “smearing” of the
368 extreme plume across the entire year and is only included to demonstrate that aerosols must be
369 modelled at spatial and temporal resolutions which can correctly model the plume. The focus of this
370 paper is on the JFM data when the anthropogenic WAP is at the most extreme levels.

371 It is worth noting that the range of AOD in the three datasets used in JFM is Terra 0.6 to 1.1,
372 MERRA-2 0.4 to 0.9 and the LME 0.3 to 1.1. The LME and MERRA-2 AOD ranges are similar
373 whilst the Terra dataset (2000 to 2019) shows a higher low value than the others as the WAP was
374 well established for the entire Terra dataset and was not for the LME and MERRA-2 data as Figure 4
375 shows.

376 Some of the correlations from the LME data show significance levels that are much less than
377 0.01 due to the correlation magnitude and the length of the time series.

378 Segment analysis results in the extraordinary correlations shown in the last two rows of
379 Figure 8 where the majority are 0.99 magnitude and these results are then discussed sequentially
380 following the hypothesis and physical model.

381 Figure 9 shows the MERRA-2 JFM segmented data analysis.

382 The comparison data in the sections below is created by subtracting the 1987 data from the
383 2004 data using either the MERRA-2 data via NASA Panoply or the NCEP/NCAR reanalysis data
384 which is sourced from the NCEP/NCAR website at [https://www.esrl.noaa.gov/psd/cgi-
385 bin/data/composites/printpage.pl](https://www.esrl.noaa.gov/psd/cgi-bin/data/composites/printpage.pl) .

386

AOD	Omega (609mb)	Surface Temp. WAP Area	Surface Pressure	Precipitation S. Europe	Precipitation UK/Ireland	Temperature N. Europe
Time Series						
Annual	0.21	-0.41	0.71	-0.63	0.26	0.30
JFM	0.72	-0.60	0.75	-0.64	0.41	0.45
Segmented						
Annual	0.96	-0.97	0.99	-0.99	0.97	0.99
JFM	0.99	-0.99	0.99	-0.99	0.97	0.98

387 Figure 8 LME correlations of AOD in the WAP Area with the parameters shown. Note:
 388 Colour coding for the correlation significance in all results is Green <0.05 and Yellow < 0.01.

389

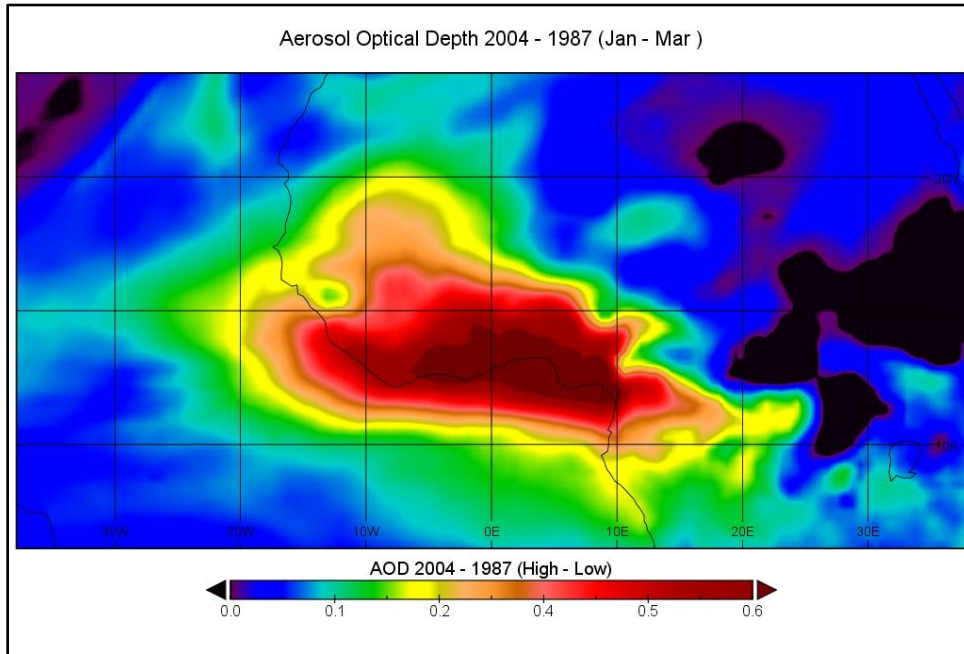
AOD	Omega (825hPa)	Surface Temp. WAP Area	Surface Pressure	Precipitation S. Europe	Precipitation UK/Ireland	Temperature N. Europe
Segmented						
JFM	0.95	-0.98	0.99	-0.99	0.92	0.98

390 Figure 9 MERRA-2 correlations of AOD in the WAP Area with the parameters shown

3.1 The WAP Forms

391 **Area used:** 0° 10°N and 0° 10°E

392 The intense WAP forms in late December and disperses in April as Figure 3 shows. Figure 10
393 shows the extreme WAP in JFM in 2004 compared to the 1987 apparition with a significant increase
394 in AOD of over 0.6 across much of the WAP Area.



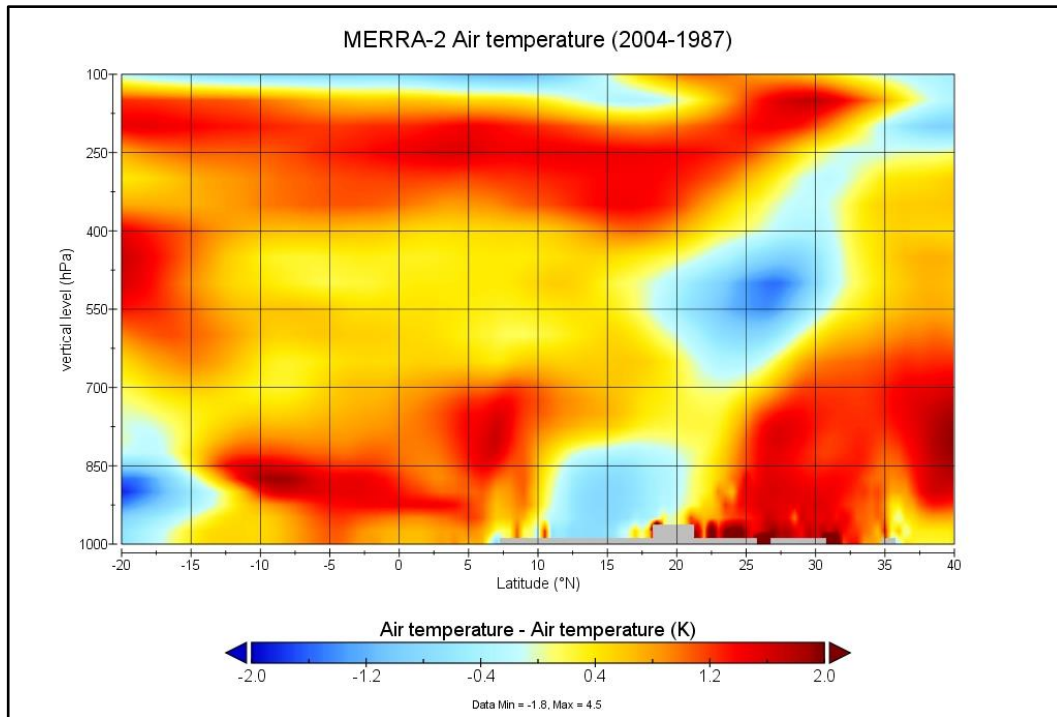
395

396 Figure 10: MERRA-2 AOD JFM 2004-1987

3.2 The WAP absorbs Solar Radiation and Heats the Atmosphere

397 **Area used:** 20°S to 40°N and 0° to 10°E

398 **Change:** Figure 11 shows the MERRA-2 air temperature averaged across the WAP Area
399 longitudes from 20°S to 40°N and it can be clearly seen that in the high AOD year the air
400 temperature within the plume at 700hPa to 850hPa is higher which correlates reasonably well with
401 estimated aerosol height from the CALIPSO data [Winker *et al.*, 2009] which on 1 January 2016 (a
402 high AOD year in the WAP Area) showed elevated aerosols at altitudes from 1.0 to 5.0 km.



403

404 Figure 11: MERRA-2 JFM Air Temperature averaged across the WAP Area Longitudes

405 2004-1987

406

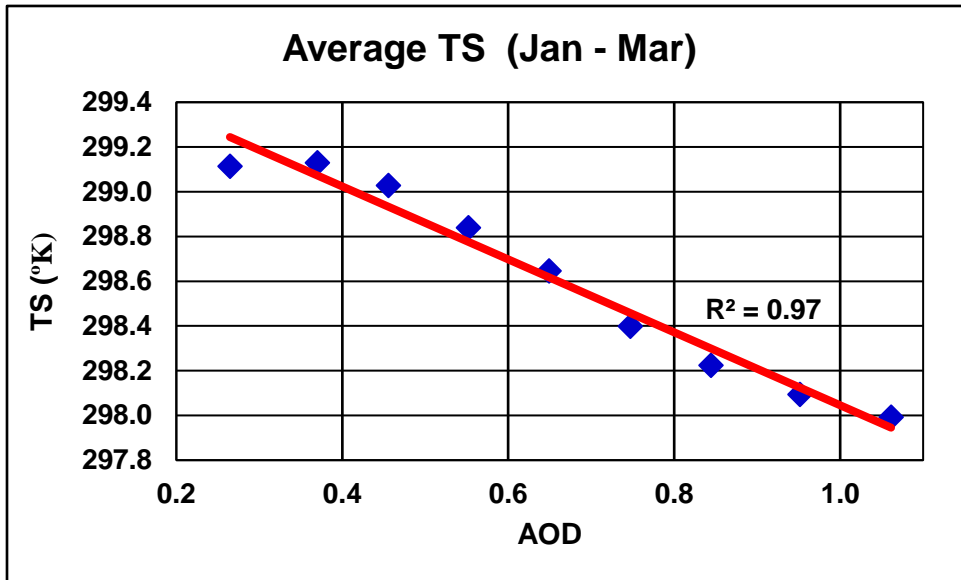
3.3 The WAP Reduces the WAP Area Surface Temperature

407 **Area used:** 0° 10°N and 0° 10°E

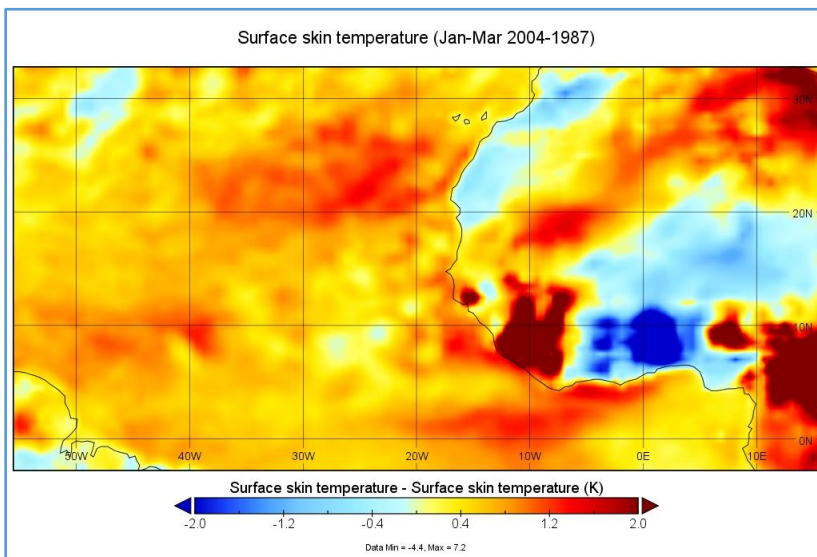
408 **Correlation:** -0.99 with r^2 values 0.97 leaving no room for other significant influences.

409 **Change:** Figure 12 shows a reduction of 1.2° K in the JFM surface temperature from
 410 the segment with the lowest AOD to the highest and Figure 13 shows the change in West Africa in
 411 JFM between 2004 and 1987 with parts of the WAP Area cooling by over 2° K.

412



413
 414 Figure 12: LME JFM Surface Temperature and WAP Area AOD. Segmented and averaged.
 415



416
 417 Figure 13: MERRA-2 Surface Skin Temperature (TS) Jan-Mar 2004 – 1987.

3.4 The WAP Reduces Convection in West Africa

418 **Area used:** 10° 15°N and 0° 10E°

419 **Correlation:** 0.99 with r^2 values 0.98 leaving no room for other significant influences.

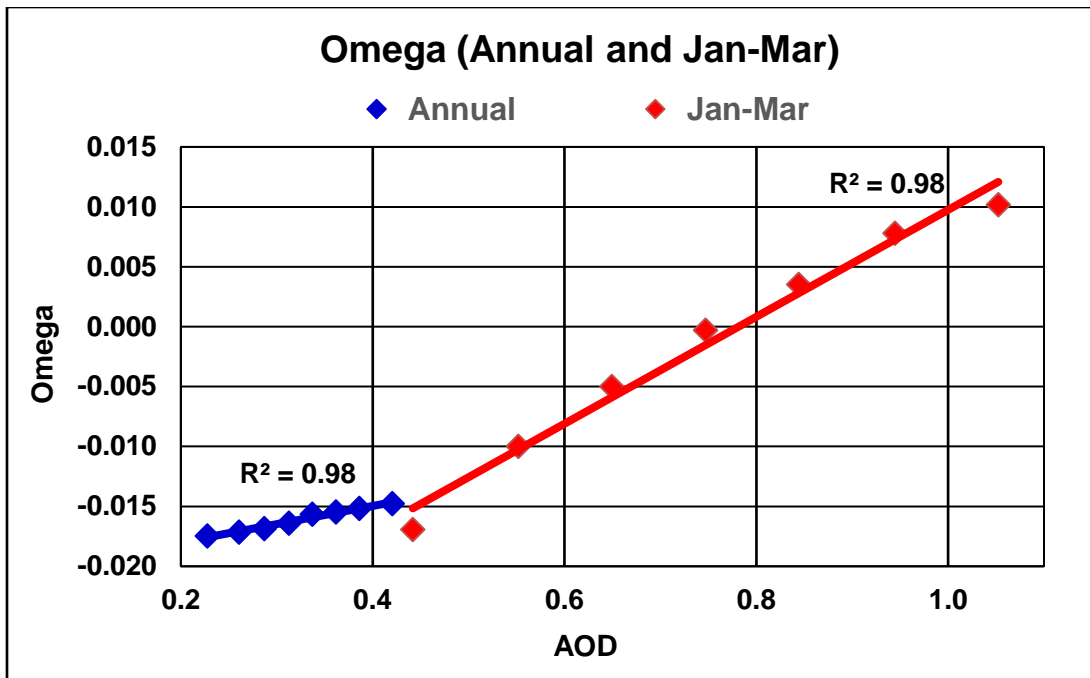
420 **Change:** Figure 14 shows an increase in JFM omega from -0.16 to 0.10 from the lowest
421 AOD to the highest implying a reduction in convection with the higher AOD levels having a positive
422 value of omega indicating that the normal convection with low AOD in West Africa has, in fact,
423 reversed.

424 **Note:** omega is pressure velocity and rising air therefore has a negative velocity as it is
425 moving from higher to lower pressure. A reduction in convection is therefore a positive change in
426 omega and as aerosols reduce convection in the WAP Area the correlations of omega and AOD are
427 positive.

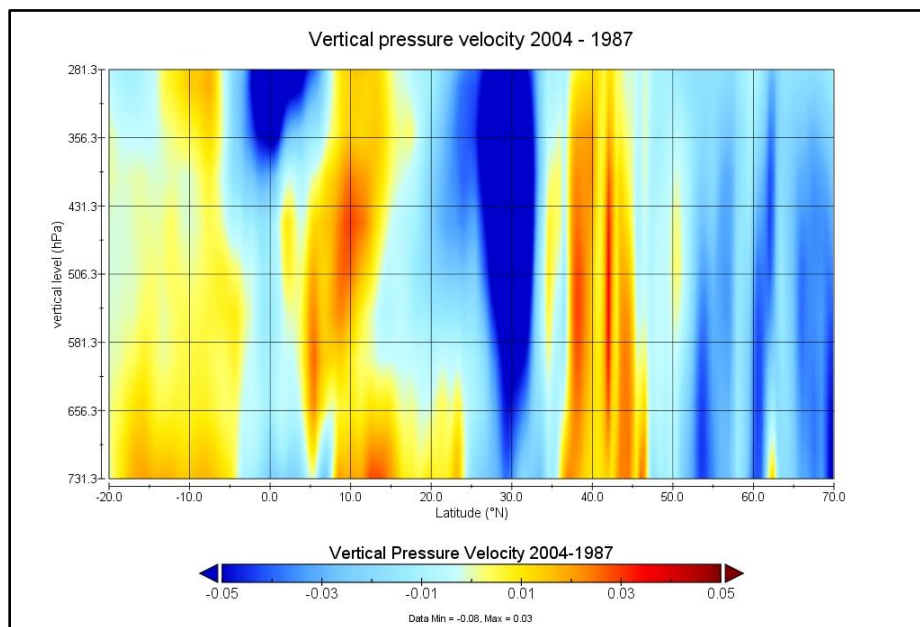
428 In Figure 14 the annual data has been included to demonstrate how averaging the effects of
429 aerosol plumes annually when the plume only exists for a few months completely destroys the
430 significant effects of the plume when it exists. The annually averaged data shows omega only rises
431 from -0.017 to -0.015 and the reversal of convection seen in the JFM data is masked by the averaging
432 process.

433 The effects of carbonaceous aerosols on convection and atmospheric circulation have been
434 extensively described in the literature as discussed in the introduction. The WAP absorbs solar
435 radiation which warms the upper atmosphere and reduces solar radiation at the surface which cools
436 the lower atmosphere. This alters the vertical temperature profile of the atmosphere with warmer air
437 above cooler air (relative to the temperatures without the plume) and this stabilises the atmosphere
438 and reduces convection. This well understood process is confirmed in the WAP Area in this paper
439 with the demonstrated correlation of omega with the AOD and in Figure 14.

440 The WAP also moves the northern Hadley Cell convection column in West Africa north as
441 Figure 15 shows where omega increases over land in West Africa where the plume exists and from
442 35 to 45 north where the anomalous high pressure over the MIEA exists.



443
444 Figure 14: LME Annual and JFM Omega and WAP Area AOD segmented and averaged



445
446 Figure 15: MERRA-2 JFM Omega 2004-1987.

447

3.5 The WAP Perturbs the Hadley Circulation:

448 The Hadley Cells are thermally driven [McGregor and Nieuwof, 1977], [Barry and Chorley,
449 2010] and [IPCC, 2007]. Reduced convection in the WAP Area alters the regional Hadley Cells and
450 this can be clearly seen in Figure 15 where the rising limb of the northern Hadley Cell has been

451 altered in the year of high AOD in the WAP Area relative to the low AOD year and the region
452 driving the greatest increase in convection is between 25° and 35° north.

3.6 The Crucial Step – The WAP Increases Surface Pressure in the MIEA

453 **Area used:** 30° 45°N and 30°W 15°E

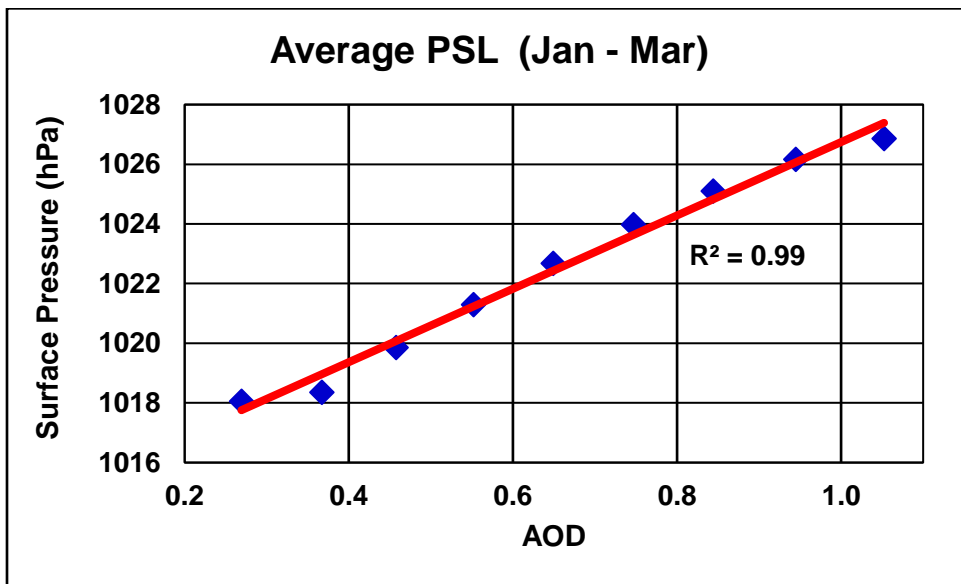
454 **Correlation:** 0.99 with r^2 values 0.99 leaving no room for other significant influences.

455 **Change:** Figure 15 shows the vertical profile of omega from 20S to 70N across the
 456 WAP Area longitudes and it is clear that a major change in omega occurs between 35N and 45N
 457 where an increase in omega in the high WAP AOD years leads to the higher pressure over the MIEA.

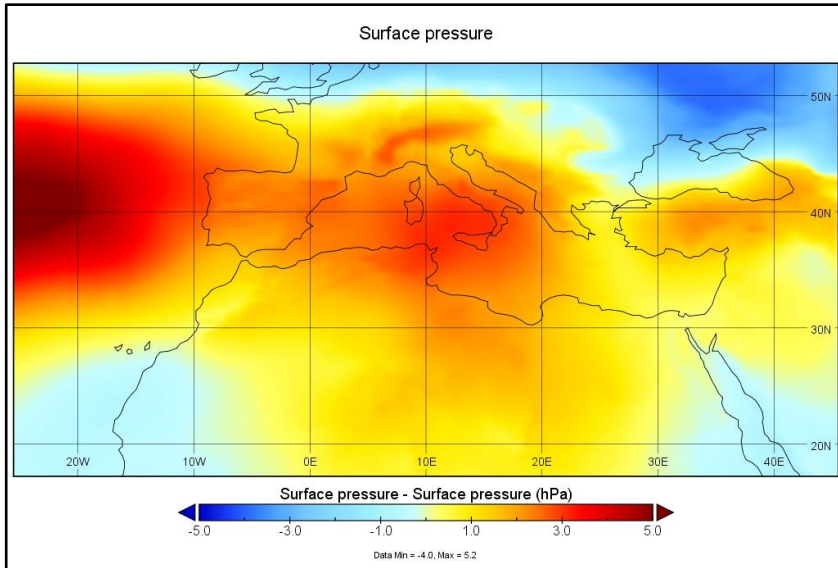
458 Figure 16 shows surface pressure rises from 1018.0 to 1026.9 hPa from the segment with the
 459 lowest AOD to the segment with the highest a rise of 8.9 hPa which is comparable to the observed
 460 increase shown in Figure 7 in [*van Oldenborgh et al.*, 2009].

461 Figure 17 shows the difference between 2004 and 1987

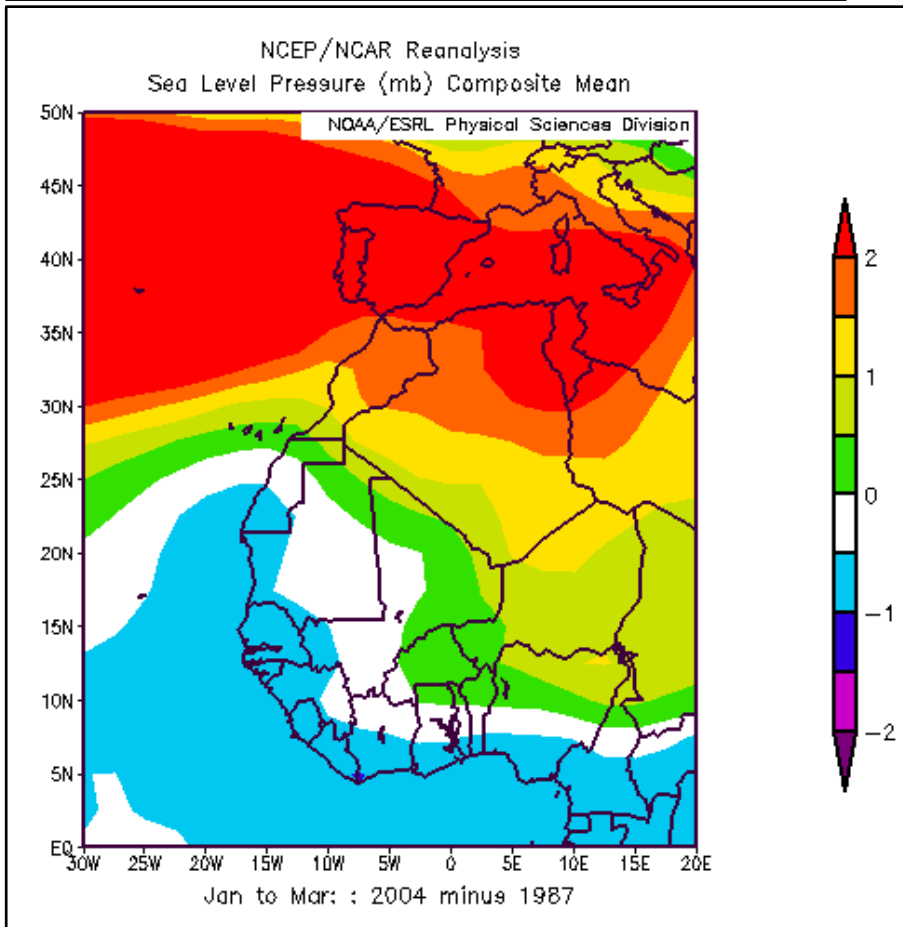
462 **Note:** This is the crucial step in the changes induced by the WAP and it is the only change
 463 remote from West Africa directly forced by the WAP with all other changes, drought in Iberia,
 464 flooding in the UK/Ireland and higher winter temperatures in northern Europe driven by this
 465 anomalous region of increased surface pressure.
 466



467
 468
 469 Figure 16: LME JFM Surface Pressure and WAP Area AOD. Segmented and averaged.
 470



471

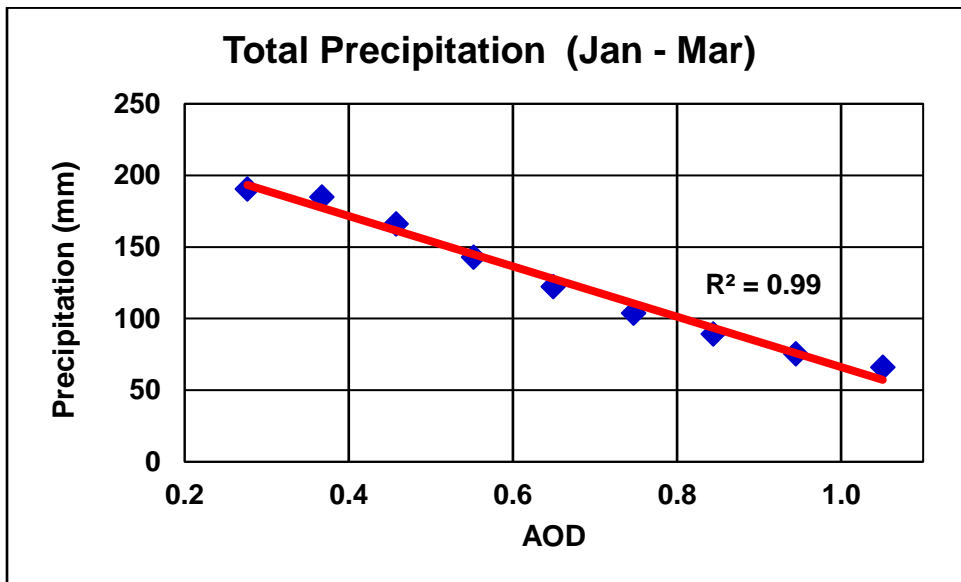


472
473
474

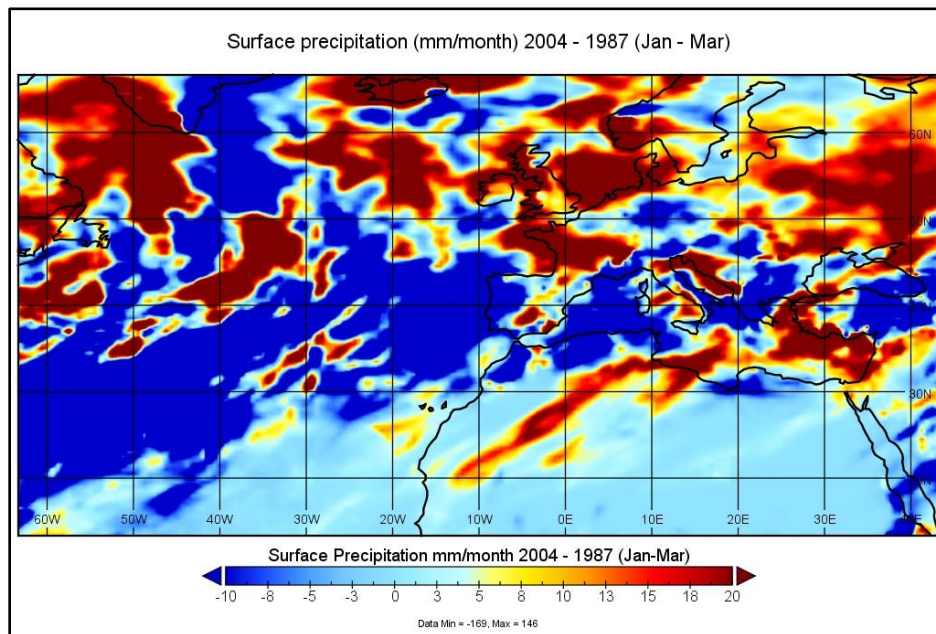
Figure 17: MERRA-2 and NCEP/NCAR Surface Pressure change 2004-1987

3.7 The WAP Reduces Precipitation in Iberia

475 **Area used:** 35° 43°N and 20°W 10°E
 476 **Correlation:** -0.99 with r^2 values 0.99 leaving no room for other significant influences.
 477 **Change:** Figure 18 shows precipitation falls from 191mm to 60 mm from the segment
 478 with the lowest AOD to the segment with the highest, a fall of 131 mm or 69% and Figure 19 shows
 479 the difference between 2004 and 1987 where most of the MIEA shows a reduction in rainfall of over
 480 8mm/month.
 481
 482



483
 484 Figure 18: LME JFM MIEA Precipitation and WAP Area AOD. Segmented and Averaged.
 485

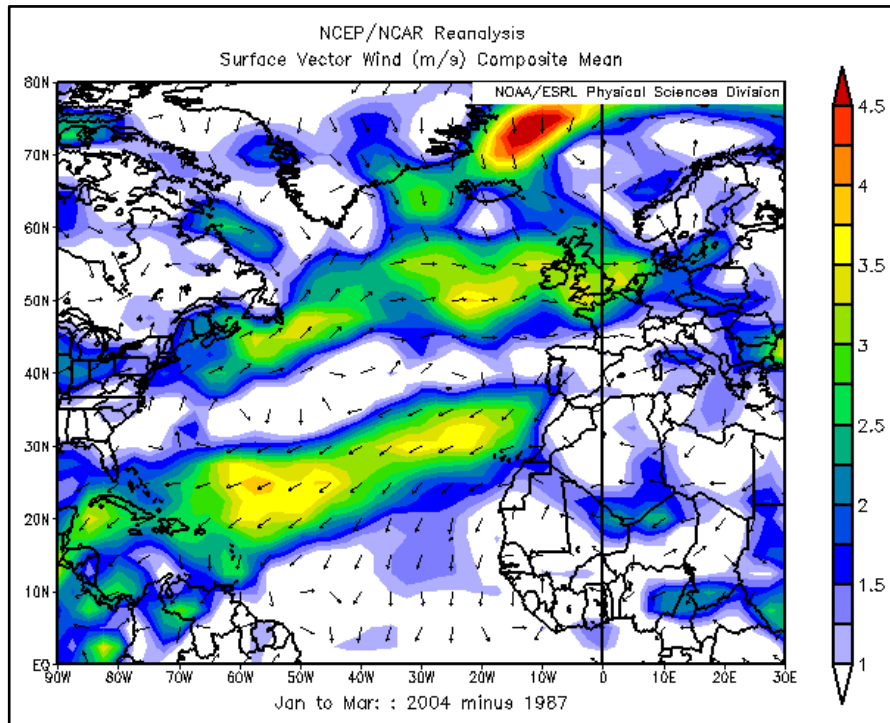


486
 487 Figure 19: MERRA-2 JFM Precipitation 2004-1987

3.8 The WAP Advects Warm, Moist Air into Northern Europe

488 With high pressure established over the MIEA, as Figure 17 shows the natural wind flows are
489 significantly perturbed as Figure 20 shows. A strong flow is visible from the Atlantic Ocean east of
490 the USA across the Atlantic and into the UK/Ireland and northern Europe. This probably constitutes
491 yet another atmospheric river, see *Ralph and Dettinger* [2011] for an early overview, [*Lavers and*
492 *Villarini*, 2013] and [*Young et al.*, 2017], carrying significant moisture from the warm ocean to the
493 UK/Ireland and northern Europe.

494



495

496

497

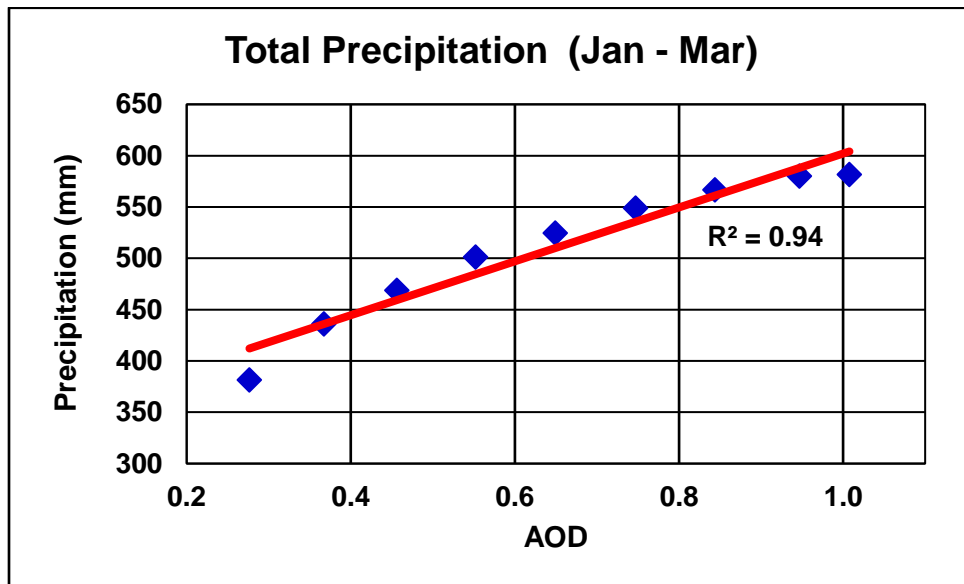
Figure 20: NCEP/NCAR JFM Surface Vector Wind 2004-1987

3.9 The WAP Increases Precipitation in the UK and Ireland

498 **Area used:** 50° 60°N and 10°W 10°E

499 **Correlation:** 0.97 with r^2 values 0.94 leaving no room for other significant influences.

500 **Change:** Figure 21 shows precipitation rises from 382 mm to 582 mm from the segment
 501 with the lowest AOD to the segment with the highest a rise of 200 mm or 52% and Figure 19 shows
 502 the difference between 2004 and 1987 with the west of England, Scotland and Northern Ireland
 503 receiving an increase in rainfall of over 20mm/month.
 504



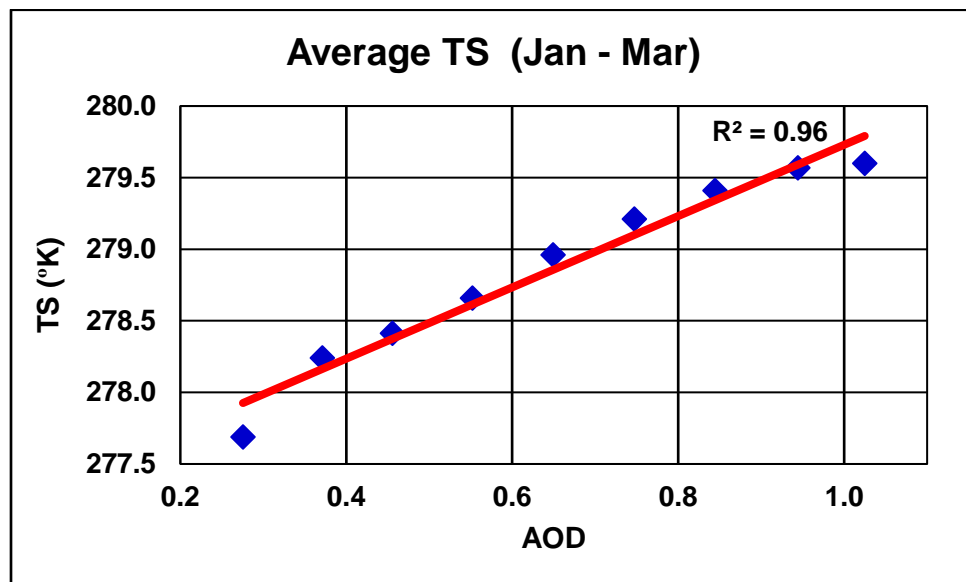
505
 506 Figure 21: LME JFM UK/Ireland Precipitation and WAP Area AOD. Segmented and averaged.
 507

3.10 The WAP Increases the Temperature in Northern Europe

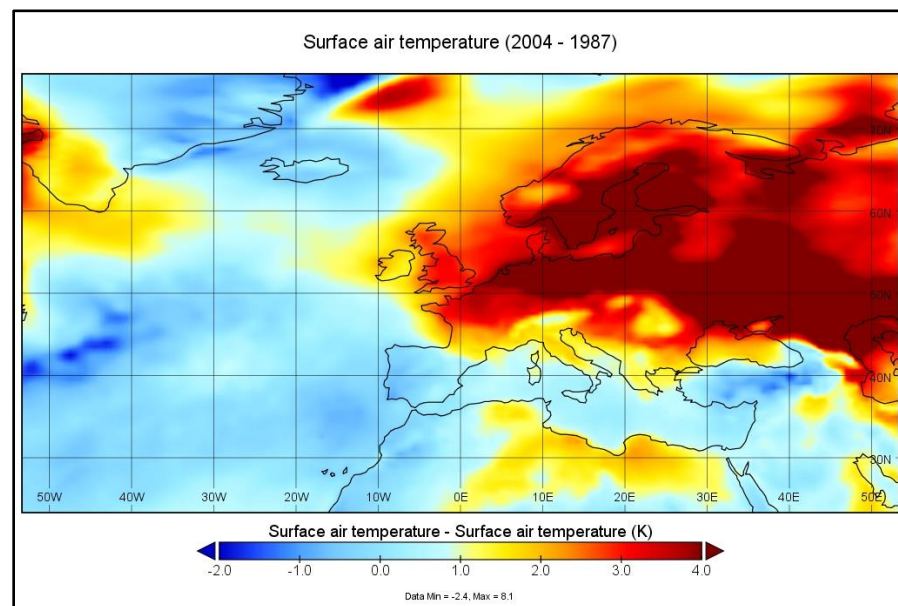
508 **Area Used:** 45° 60°N and 15°W 30°E

509 **Correlation:** 0.98 with r^2 values 0.96 leaving no room for other significant influences.

510 **Change:** Figure 22 shows the temperature in northern Europe rises from 277.7° K to
 511 279.6° K from the segment with the lowest AOD to the segment with the highest a rise of 1.9 ° K.
 512 and Figure 23 shows the difference between 2004 and 1987 where significant parts of Europe north
 513 of the Alps including Scandinavia show rises of over 4° K in the year of high WAP Area AOD.
 514



515
 516 Figure 22: LME JFM Northern European Temperatures and WAP Area AOD. Segmented and
 517 averaged
 518



519
 520 Figure 23: MERRRA-2 Surface Temperature 2004 - 1987

4 CAUSATION ANALYSIS

521 It is clearly understood that correlation between events A and B does not prove causation
522 from A to B or vice versa. Thus, the causal relationship between the WAP and the European climate
523 must be demonstrated in other ways.

4.1 Analysis without Correlation

524 Figure 18 shows that the LME JFM precipitation in Iberia falls from 191 mm to 60 mm a fall
525 of 69% from the segment with the lowest AOD to the one with the highest and this is comparable to
526 the fall in the measured Iberian rainfall in the 2004/05 water year of -60% [*García-Herrera et al.*,
527 2007]without using correlation.

4.2 Modelling

528 **LME:** there is no physical mechanism by which drought or SLP in Iberia can create aerosols
529 in the LME over West Africa hence the causal direction must run from the aerosols to the rainfall and
530 SLP.

531 In addition, the aerosol forcings in all LME runs are fixed at 1850 values except for the
532 “ozone and aerosol” and “all” runs and there can therefore be no forcing of the aerosols by any agent
533 within these six runs and the causal direction must flow from the aerosols to the rainfall and SLP.

534 **MERRA-2** reanalysis assimilates measured aerosol data and therefore the causal direction
535 must be from the aerosols to the rainfall and SLP as it cannot be the reverse.

4.3 Multiple Independent Datasets

536 The eight LME modelling runs and the MERRA-2 reanalysis exhibit very low or negative
537 correlations between the WAP AOD in the individual runs as shown in the correlation matrix in
538 Appendix B with an overall average 0.0016. Hence the datasets are independent.

539 All the eight segmented LME and the MERRA-2 datasets show correlations at magnitude
540 0.98 or greater with the Iberian rainfall and MIEA SLP at significance of <0.01 or less and the
541 chance that all these nine independent datasets show the same result and are wrong is the product of
542 the significance i.e. 0.01^{-9} or 10^{-18} , a vanishingly small number.

4.4 Segmented Data

543 The climate is a chaotic system and my preferred way to analyse climate data is to segment,
544 average the data as the averaging process will improve the signal to noise ratio of the analysis. When
545 the LME WAP JFM AOD and rainfall and SLP data in Iberia and the MIEA is segmented on the
546 basis of the AOD data and then averaged and correlated R^2 values of 0.99 (Figure 16 and 18) are
547 found. This demonstrates clearly that the WAP is the major and possibly the only driver of reduced
548 winter rainfall and increased SLP in Iberia and the MIEA.

549 The difference between the lowest LME WAP Area AOD segment and the highest shows a
550 reduction in JFM precipitation in Iberia of 131 mm or 69% in Figure 18 with an obvious, well-
551 established trend. Similarly, Figure 16 shows and increase in SLP of 8.9 hPa also with a well-
552 established trend.

553 This analysis does not depend on correlation.

4.5 Another Event “C”

554 One possible explanation for the correlations shown in this paper is that another unknown
555 event “C” causes the WAP all the other effects discussed in this paper simultaneously.

556 However, Appendix A shows the JFM WAP is unquestionably anthropogenic and caused by
557 biomass burning in deliberately lit fires in West Africa and it is therefore impossible for another
558 event to cause the WAP and this possibility must be rejected.

4.6 Causal Direction

559 Therefore with:

- 560 1. The segmented LME data showing an increase in pressure in the MIEA as the AOD level of
561 the WAP rises without using correlation
- 562 2. The segmented LME data showing a reduction in rainfall in Iberia as the AOD level of the
563 WAP rises without using correlation;
- 564 3. The segmented LME data showing an increase in rainfall in the UK/Ireland as the AOD level
565 of the WAP rises without using correlation;
- 566 4. The segmented LME data showing an increase in temperature in northern Europe as the AOD
567 level of the WAP rises without using correlation;
- 568 5. The LME time series analysis showing the same results across multiple independent datasets
569 with a vanishingly small chance of error;
- 570 6. The LME data showing, by a preferred analysis method, extremely high correlations of AOD
571 with surface pressure, precipitation and temperature which leave no possibility of other
572 significant drivers;
- 573 7. The MERRA-2 data confirming the LME data;

574 the inevitable conclusion is that the hypothesis is proven and the WAP is the primary driver
575 in JFM of increased: pressure over the MIEA; rainfall in the UK/Ireland; and temperature in northern
576 Europe and reduced rainfall in Iberia and, based on r^2 values, is the sole driver.

5 FUTURE RESEARCH

5.1 Confirming the conclusions

577 To finally confirm the findings above I suggest that a further LME style analysis is
578 undertaken in which an aerosol plume is created in the model which ramps up from the naturally low
579 level which existed in 1950 in December to reach the same AOD and geographic extent as the
580 extreme JFM WAP of 2004 in January, continues at the same level to March and ramps down in
581 April to the naturally low level which existed in May 1950. This plume to be applied in the model
582 with random returns from 3 to 10 years to mimic the return frequency of high AOD events in Figure
583 4 with all other forcing agents held constant.

584 This modelling should be repeated with AOD levels reduced by perhaps 50% between runs to
585 determine the level of AOD in the WAP Area which is required to create the effects demonstrated in
586 this paper.

587 These experiments will confirm the analysis in this paper and provide the information
588 governments will require to undertake the actions needed to reduce the WAP AOD to levels which
589 will not impact the winter climate of Europe and will allow it to return to its natural state without the
590 anthropogenic influence of the WAP.

5.2 Mitigating the WAP

591 5.2.1 Seasonal Biomass Burning

592 The most significant source of aerosols in the WAP is biomass burning which takes place
593 towards the end of the dry season in West Africa in JFM. The biomass is burned for the reasons
594 outlined in the Appendix.

595 Reducing the incidence of biomass burning requires the deployment of new technologies
596 which are now available to take the unwanted biomass and convert it into useful products such as
597 liquid fuel which, of course, would be carbon dioxide neutral as the feedstock is not a fossil fuel.
598 MIT in 2015 produced a report into this technology: Biomass to Liquid Fuels Pathways [Seifkar et
599 al., 2015] and there are many others such as [Graham *et al.*, 2011].

600 Deployment of this technology would enable the rapid reduction of in the AOD levels over
601 West Africa as the technology would create a new income stream for farmers and others selling into
602 a new industry and it would enable West African governments to ban biomass burning in the open as
603 other governments have done.

604 5.2.2 Gas Flares

605 The anthropogenic WAP also comprises carbonaceous aerosols from the routine flaring of
606 associated gas in the oil production industry. (Associated gas is gas dissolved in liquid oil which
607 boils out of the liquid when the oil is produced from deep in the Earth (typically 1,500 to 3,000
608 metres depth) and the pressure reduces to atmospheric levels. Associated gas produced in areas
609 without infrastructure to use the gas is flared. A process which is, indubitably, wasteful.)

610 The World Bank via the GGFRP has been trying to reduce routine flaring in the oil industry
611 with some success in West Africa with the amount of gas flared in Nigeria reducing from 8.4 to 7.4
612 billion cubic metres (bcm) between 2014 and 2018 according the GGFRP website at
613 <https://www.worldbank.org/en/programs/gasflaringreduction#7> .

614 Even with this success the oil industry still flares a significant amount of gas in Nigeria which
615 in 2018 was the 7th largest flaring country in the World and the industry should be required to
616 immediately eliminate the routine flaring of gas by government or, at a minimum, flare the gas
617 without creating aerosols.

618 5.2.3 Background AOD Levels

619 The background AOD level refers to the average level between May and November a period
620 when extreme biomass burning cannot occur due to the West African monsoon.

621 The representative concentration pathway data from the International Institute for Applied
622 Systems Analysis (IIASA) at
623 <https://www.iiasa.ac.at/web/home/research/researchPrograms/TransitionstoNewTechnologies/RCP.e>
624 [n.html](https://www.iiasa.ac.at/web/home/research/researchPrograms/TransitionstoNewTechnologies/RCP.e) shows no change in carbonaceous aerosols from the MAF area (Middle East and Africa)
625 before 1950 and then a six fold increase by 2000 with the majority of the increase occurring by 1970.
626 Hence as West Africa is one of the regions where there has been a significant increase it is obvious
627 that the WAP Area background AOD level in 1950 must have been significantly lower than the 1980
628 level shown in Figure 4. It is therefore possible that this increased background level since 1950 may
629 have also affected the climate of Europe in other seasons and this requires further research.

5.3 Other Aerosol Plumes

630 Eight continental scale aerosol plumes now exist in the World each year, each in its own
631 season. They can be seen in [Potts, 2017], a poster from the American Geophysical Union Fall
632 Meeting in 2017, available from the Earth and Space Science Open Archive.

633 My future research on the annual apparitions of anthropogenic, continental scale, aerosol
634 plumes will focus on the seasonal effects of the other plumes on the climate of Europe in summer
635 and autumn, on Australian drought, and on ENSO.

636 6 CONCLUSIONS

637 The LME with 1.156 years of data and MERRA-2 with 40 years of data confirm the direct
638 connection between the WAP and the European winter climate in multiple independent ways and my
639 analysis clearly shows that the relationship must be causal.

640 I therefore conclude that:

- 641 1. The hypothesis is proven and that Aerosol Regional Dimming by apparitions of the WAP
642 is the prime trigger for and sustaining influence on the winter climate of Europe driving
643 increased pressure over the MIEA which then creates drought in Iberia, increased rainfall
644 in the UK/Ireland and increased temperatures in northern Europe.
- 645 2. The reason that the climate modelling cited in the introduction failed to replicate the
646 significant observed surface pressure rise over the Mediterranean is, of course, that the
647 models did not accurately incorporate the carbonaceous, anthropogenic aerosols of the
648 WAP.
- 649 3. The WAP and the other seven continental scale aerosol plumes which now exist each
650 year, each in its own season, must be accurately incorporated in climate models at spatial
651 and temporal resolutions that do not lose the effects of the plumes due to averaging. I
652 suggest a spatial resolution of less than 2° of latitude and longitude and a temporal
653 resolution of less than 1 month are required to do this.
- 654 4. With the proof that the WAP changes the climate of Europe 40 to 50 degrees of latitude
655 away it is obviously possible that the other seven continental scale aerosol plumes will
656 have effects which are even more remote from the plume than the WAP is from Europe
657 and this requires investigation.

658 Finally I concur with *Booth et al.* [2012] that emissions of carbonaceous aerosols are directly
659 addressable by government policy actions and suggest that this is an urgent necessity to restore the
660 winter climate of Europe to its pre-WAP, natural state circa 1950.

661 7 DATA Sources

662 The following data was used:

- 663 NASA MERRA-2 <https://giovanni.gsfc.nasa.gov/giovanni/>
664 NASA Terra <https://giovanni.gsfc.nasa.gov/giovanni/>
665 NASA Fire Data <https://earthdata.nasa.gov/earth-observation-data/near-real-time/firms/active-fire-data> ;
666
667 NASA CALIPSO Data https://eosweb.larc.nasa.gov/project/calipso/calipso_table .
668 NOAA/ESRL images <http://www.esrl.noaa.gov/psd/> .
669 LME <https://www.earthsystemgrid.org/>
670 The UK Met Office at <https://www.metoffice.gov.uk/weather/learn-about/past-uk-weather-events>
671
672 The IPCC Reports <https://www.ipcc.ch/reports/>
673 Google Earth <https://www.google.com/earth/>
674 Forest loss data <https://www.globalforestwatch.org/>
675 BP oil production data <https://www.bp.com/en/global/corporate/energy-economics/statistical-review-of-world-energy.html>
676
677 The GGFRP <https://www.worldbank.org/en/programs/gasflaringreduction> ;
678 The GVP <http://dx.doi.org/10.5479/si.GVP.VOTW4-2013> ;
679 UN Population Data
680 <https://www.un.org/en/development/desa/population/publications/database/index.asp>
681

682 **8 APPENDIX A - SOURCES OF THE WEST AFRICAN AEROSOL PLUME**

683 The major sources of aerosols in West Africa are biomass burning and gas flares in the oil
684 production industry. Volcanoes are a minor source and are not significant in this region.

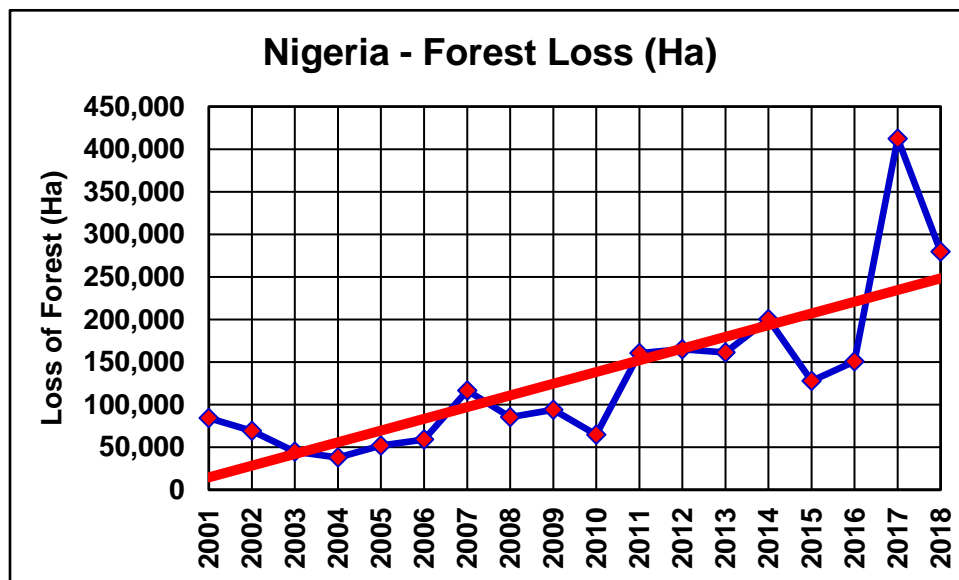
8.1 Biomass Burning

685 Biomass burning in West Africa is a large direct source of carbonaceous aerosols and is part
686 of the traditional annual agricultural cycle. It occurs during the dry season before the start of the local
687 monsoon in April. The level of biomass burning in the region has increased significantly in recent
688 decades and is expected to continue to increase [Knippertz *et al.*, 2015].

689 In the WAP Area the biomass burning aerosol plume is at its most intense in JFM as Figure 3
690 shows. The increase in biomass burning in the WAP Area in recent decades has been driven by the
691 increasing population of the WAP Area. The population of West Africa has increased from 71 to 307
692 million between 1950 and 2010 and is expected to increase to 796 million by 2050. An elevenfold
693 increase in 100 years (United Nations
694 <https://www.un.org/en/development/desa/population/publications/database/index.asp>). This
695 increasing population has forced: an increase in food production from tropical agriculture with its
696 attendant smoke/aerosols; and increased rainforest clearing to provide living space and agricultural
697 land.

698 A major source of aerosols in West Africa is forest clearing in Nigeria, the country at the
699 centre of the WAP. Data from The Global Forest Watch at <https://www.globalforestwatch.org/>
700 [Hansen *et al.*, 2013] was downloaded and Figure 24 shows the annual forest loss which has trended
701 from under 50,000 Ha in 2001 to 250,000 in 2018 a fivefold increase.

702



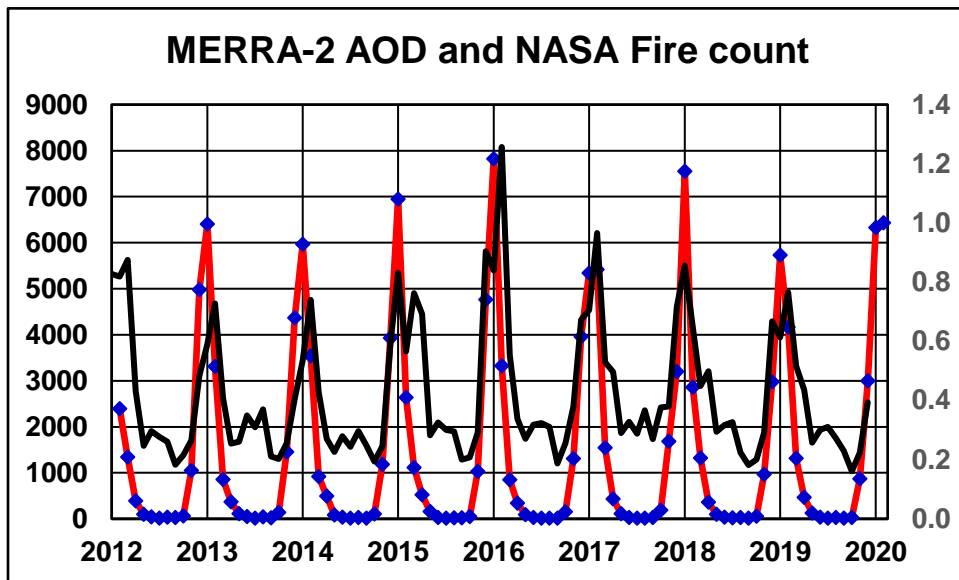
703

704

Figure 24: Annual Forest Loss in Nigeria

705

706 The archived active fires from Feb 2012 to Feb 2020 from NASA at
 707 <https://earthdata.nasa.gov/earth-observation-data/near-real-time/firms/active-fire-data>
 708 was downloaded for the area 5° to 15°N 0° to 10°E. Over 3.8 million observations for this area are
 709 included in the database. The data was summed for each day and the daily total then averaged for
 710 each month to avoid double counting fires which are recognized on more than one day. The fire data
 711 and MERRA-2 AOD are plotted in Figure 25 to show the close connection between fire and AOD in
 712 West Africa which is also shown in the high correlation (0.75 significance <0.01) between the AOD
 713 and fire numbers in this period.



714
 715 Figure 25: West African Archived Fires (NASA) and NASA MERRA-2 WAP Area AOD.
 716

717 Together the literature, burned area and fire data show that the extreme AOD in JFM is
 718 created by fire in West Africa and the WAP is therefore predominantly carbonaceous.
 719

8.2 Gas Flares

720 Gas Flares in the oil production industry increased in number over recent decades as oil
721 production in West Africa increased from 274,000 to 2,342,000 barrels of oil per day between 1965
722 and 2018 (BP Statistical Review of World Energy 2019) with the majority of the increase occurring
723 before 1974. Nigeria is the major producer in the region with 88% of the total oil production in West
724 Africa.

725 The World Bank has established the GGFRP which estimates Nigeria flares 7.4 billion m³ of
726 natural gas each year and the gas flare locations are shown in Figure 7. NOAA identifies 359 flare
727 locations in West Africa from Congo to Mauretania with Nigeria hosting the majority at 203. Images
728 of such flares producing aerosols are easily found e.g. Figure 26 from NOAA or at the GGFRP web
729 site.

730



731

732 Figure 26: Gas Flare NOAA at https://ngdc.noaa.gov/eog/viirs/download_global_flare.html

8.3 Volcanoes

733 The GVP database of volcanic eruptions [Venzke, 2013] shows that the WAP Area hosts
734 several volcanoes with only one. Mount Cameroon, recently active with an estimated 18 months of
735 activity since 1900 with volcanic explosivity indices of 1 or 2. As this is unlikely to have any
736 significant impact on the effects discussed in this paper an analysis of volcanic activity has not been
737 included in this paper.

738 **Note:** this section on volcanoes is included for completeness as in some regions volcanic
739 activity is a major source of aerosols and a negative finding should be reported.

740

9 APPENDIX B – CORRELATION MATRIX FOR LME AND MERRA-2

	850	All	Aero	GHG	Land	Orbital	Solar	Volc	MERRA-2	Average
850	1.00	0.03	-0.02	0.02	-0.02	-0.01	0.05	-0.01	-0.12	-0.01
All	0.03	1.00	-0.03	0.01	0.00	-0.02	-0.02	-0.02	0.14	0.01
Aero	-0.02	-0.03	1.00	0.01	-0.07	0.06	-0.09	-0.01	-0.08	-0.03
GHG	0.02	0.01	0.01	1.00	0.02	0.01	-0.03	0.03	0.04	0.01
Land	-0.02	0.00	-0.07	0.02	1.00	-0.01	0.01	-0.03	-0.07	-0.02
Orbital	-0.01	-0.02	0.06	0.01	-0.01	1.00	-0.04	0.03	0.23	0.03
Solar	0.05	-0.02	-0.09	-0.03	0.01	-0.04	1.00	-0.06	0.14	0.00
Volc	-0.01	-0.02	-0.01	0.03	-0.03	0.03	-0.06	1.00	-0.26	-0.04
MERRA-2	-0.12	0.14	-0.08	0.04	-0.07	0.23	0.14	-0.26	1.00	0.00
Average	-0.01	0.01	-0.03	0.01	-0.02	0.03	0.00	-0.04	0.00	0.00

741

742 Figure 27: Correlation matrix for LME and MERRA-2 WAP Area AOD/AOD. The average
 743 excludes the self-correlations which return 1.00.

744

745 **Note:** There are some small correlations between MERRA-2 AOD and the LME runs however some
 746 are positive and some negative in Figure 27 hence the 9 data sets are independent.

747 **ACKNOWLEDGEMENTS**

748 I acknowledge:

749 NASA: Analyses and visualizations used in this paper were produced with the Giovanni
750 online data system, developed and maintained by the NASA GES DISC; the mission scientists and
751 Principal Investigators who provided the data and images used in this paper including the MERRA-2
752 data; and Dr Robert Schmunk for the Panoply data viewer;

753 NASA for the fire data at <https://earthdata.nasa.gov/earth-observation-data/near-real-time/firms/active-fire-data> ;

755 NASA for the CALIPSO data obtained from the NASA Langley Research Center
756 Atmospheric Science Data Center at https://eosweb.larc.nasa.gov/project/calipso/calipso_table .

757 The NOAA/ESRL Physical Sciences Division, Boulder Colorado for the images from their
758 Web site at <http://www.esrl.noaa.gov/psd/> .

759 The CESM1(CAM5) Last Millennium Ensemble Community Project and supercomputing
760 resources provided by NSF/CISL/Yellowstone;

761 The UK Met Office at <https://www.metoffice.gov.uk/weather/learn-about/past-uk-weather-events>
762 [events](https://www.metoffice.gov.uk/weather/learn-about/past-uk-weather-events) for the UK flood information;

763 The IPCC for the images from Assessment Report Four;

764 Google Earth™ and the copyright holders noted on the image for the image of the Earth;

765 The United Nations Department of Economic and Social Affairs Population Division for the
766 world population statistics at
767 <https://www.un.org/en/development/desa/population/publications/database/index.asp>;

768 The Global Forest Watch at <https://www.globalforestwatch.org/> for the forest loss data;

769 BP for the oil production statistics at <https://www.bp.com/en/global/corporate/energy-economics/statistical-review-of-world-energy.html>

771 The Global Gas Flaring Reduction Partnership (World Bank and NOAA) for the gas flare
772 data and image of a flare at <https://www.worldbank.org/en/programs/gasflaringreduction> ;

773 The Global Volcanism Program at the Smithsonian Institution for the volcano eruption data.
774 <http://dx.doi.org/10.5479/si.GVP.VOTW4-2013> ;

775 All data supporting the conclusions is available from the sources noted in the text.

776 This research project was funded personally by the author and his wife Julie.

777 **References**

- 778 Allen, R. J., S. C. Sherwood, J. R. Norris, and C. S. Zender (2012), Recent Northern Hemisphere tropical expansion
779 primarily driven by black carbon and tropospheric ozone, *Nature*, *485*(7398), 350-354, doi:10.1038/nature11097.
- 780 Barry, R. G., and R. J. Chorley (2010), *Atmosphere Weather and Climate* Routledge, Abingdon UK.
- 781 Booth, B. B., N. J. Dunstone, P. R. Halloran, T. Andrews, and N. Bellouin (2012), Aerosols implicated as a prime driver
782 of twentieth-century North Atlantic climate variability, *Nature*, *484*(7393), 228-232, doi:10.1038/nature10946.
- 783 Cattiaux, J., R. Vautard, C. Cassou, P. Yiou, V. Masson-Delmotte, and F. Codron (2010), Winter 2010 in Europe: A cold
784 extreme in a warming climate, *Geophysical Research Letters*, *37*(20), doi:10.1029/2010gl044613.
- 785 Duncan, B. N., I. Bey, M. Chin, L. J. Mickley, T. D. Fairlie, R. V. Martin, and H. Matsueda (2003), Indonesian wildfires
786 of 1997: Impact on tropospheric chemistry, *Journal of Geophysical Research: Atmospheres*, *108*(D15), 4458,
787 doi:10.1029/2002JD003195.
- 788 Forster, P., et al. (2007), Changes in Atmospheric Constituents and in Radiative Forcing. In: *Climate Change 2007: The*
789 *Physical Science Basis. Contribution of Working Group I to the Fourth Assessment Report of the Intergovernmental*
790 *Panel on Climate Change* [Solomon, S., D. Qin, M. Manning, Z. Chen, M. Marquis, K.B. Averyt, M. Tignor and H.L.
791 Miller (eds.)] Cambridge University Press, Cambridge, United Kingdom and New York, NY, USA.
- 792 García-Herrera, R., D. Paredes, R. M. Trigo, I. F. Trigo, E. Hernández, D. Barriopedro, and M. A. Mendes (2007), The
793 Outstanding 2004/05 Drought in the Iberian Peninsula: Associated Atmospheric Circulation, *Journal of*
794 *Hydrometeorology*, *8*(3), 483-498, doi:10.1175/jhm578.1.
- 795 Gelaro, R., et al. (2017), The Modern-Era Retrospective Analysis for Research and Applications, Version 2 (MERRA-2),
796 *Journal of Climate*, *30*(14), 5419-5454, doi:10.1175/jcli-d-16-0758.1.
- 797 Graham, P. W., T. S. Brinsmead, and L. J. Reedman² (2011), An assessment of competition for biomass resources within
798 the energy and transport sectors *Rep.*, CSIRO.
- 799 Hansell, R. A., S. C. Tsay, Q. Ji, K. N. Liou, and S. C. Ou (2003), Surface aerosol radiative forcing derived from
800 collocated ground-based radiometric observations during PRIDE, SAFARI, and ACE-Asia, *Appl Opt*, *42*(27), 5533-5544.
- 801 Hansen, M. C., et al. (2013), High-Resolution Global Maps of 21st-Century Forest Cover Change, *Science*, *342*(6160),
802 850-853, doi:10.1126/science.1244693.
- 803 Hegerl, G. C., F. W. Zwiers, P. Braconnot, N. P. Gillett, Y. Luo, J. A. Marengo Orsini, N. Nicholls, J. E. Penner, and P.
804 A. Stott (2007), Understanding and Attributing Climate Change. In: *Climate Change 2007: The Physical Science Basis.*
805 *Contribution of Working Group I to the Fourth Assessment Report of the Intergovernmental Panel on Climate Change*
806 [Solomon, S., D. Qin, M. Manning, Z. Chen, M. Marquis, K.B. Averyt, M. Tignor and H.L. Miller (eds.)]. Cambridge
807 University Press, Cambridge, United Kingdom and New York, NY, USA.
- 808 Huntingford, C., et al. (2014), Potential influences on the United Kingdom's floods of winter 2013/14, *Nature Clim.*
809 *Change*, *4*(9), 769-777, doi:10.1038/nclimate2314.
- 810 IPCC (2007), IPCC Assessment Report 4 Glossary.
- 811 Kalnay, E., et al. (1996), The NCEP/NCAR 40-Year Reanalysis Project, *Bulletin of the American Meteorological*
812 *Society*, *77*(3), 437-471, doi:10.1175/1520-0477(1996)077<0437:TNYRP>2.0.CO;2.
- 813 Kaufman, Y. J., B. N. Holben, D. Tanré, I. Slutsker, A. Smirnov, and T. F. Eck (2000), Will aerosol measurements from
814 Terra and Aqua Polar Orbiting satellites represent the daily aerosol abundance and properties?, *Geophysical Research*
815 *Letters*, *27*(23), 3861-3864, doi:10.1029/2000GL011968.
- 816 Kirchstetter, T. W. (2004), Evidence that the spectral dependence of light absorption by aerosols is affected by organic
817 carbon, *Journal of Geophysical Research*, *109*(D21), doi:10.1029/2004jd004999.
- 818 Knippertz, P., M. J. Evans, P. R. Field, A. H. Fink, C. Lioussé, and J. H. Marsham (2015), The possible role of local air
819 pollution in climate change in West Africa, *Nature Clim. Change*, *5*(9), 815-822, doi:10.1038/nclimate2727.
- 820 Lamarque, J. F., et al. (2010), Historical (1850–2000) gridded anthropogenic and biomass burning emissions of reactive
821 gases and aerosols: methodology and application, *Atmospheric Chemistry and Physics*, *10*(15), 7017-7039,
822 doi:10.5194/acp-10-7017-2010.
- 823 Lavers, D. A., and G. Villarini (2013), The nexus between atmospheric rivers and extreme precipitation across Europe,
824 *Geophysical Research Letters*, *40*(12), 3259-3264, doi:10.1002/grl.50636.
- 825 Levy II, H., D. T. Shindell, A. Gilliland, M. D. Schwarzkopf, and L. W. Horowitz (2008), Executive Summary in
826 *Climate Projections Based on Emissions Scenarios for Long-Lived and Short-Lived Radiatively Active Gases and*
827 *Aerosols*. H. Levy II, D.T. Shindell, A. Gilliland, M.D. Schwarzkopf, L.W. Horowitz, (eds.). A Report by the U.S.
828 Climate Change Science Program and the Subcommittee on Global Change Research, Washington, D.C.
- 829 Luterbacher, J., M. A. Liniger, A. Menzel, N. Estrella, P. M. Della-Marta, C. Pfister, T. Rutishauser, and E. Xoplaki
830 (2007), Exceptional European warmth of autumn 2006 and winter 2007: Historical context, the underlying dynamics, and
831 its phenological impacts, *Geophysical Research Letters*, *34*(12), doi:10.1029/2007gl029951.

- 832 McGregor, G. R., and S. Nieuwof (1977), *Tropical Climatology*, 207 pp., John Wiley and Sons.
- 833 Menon, S., J. Hansen, L. Nazarenko, and Y. Luo (2002), Climate Effects of Black Carbon Aerosols in China and India,
834 *Science*, 297(5590), 2250-2253, doi:10.1126/science.1075159.
- 835 Novakov, T., V. Ramanathan, J. E. Hansen, T. W. Kirchstetter, M. Sato, J. E. Sinton, and J. A. Sathaye (2003), Large
836 historical changes of fossil-fuel black carbon aerosols, *Geophysical Research Letters*, 30(6), 1324,
837 doi:10.1029/2002GL016345.
- 838 Oluleye, A., K. O. Ogunjobi, A. Bernard, V. O. Ajayi, and A. A. A. (2012), Multiyear Analysis of Ground-Based
839 Sunphotometer (AERONET) Aerosol Optical Properties and its Comparison with Satellite Observations over West
840 Africa, *Global Journal of HUMAN SOCIAL SCIENCE Geography & Environmental GeoSciences*, 12(10).
- 841 Osborn, T. J. (2004), Simulating the winter North Atlantic Oscillation: the roles of internal variability and greenhouse gas
842 forcing, *Climate Dynamics*, 22(6-7), doi:10.1007/s00382-004-0405-1.
- 843 Ott, L., B. Duncan, S. Pawson, P. Colarco, M. Chin, C. Randles, T. Diehl, and E. Nielsen (2010), Influence of the 2006
844 Indonesian biomass burning aerosols on tropical dynamics studied with the GEOS-5 AGCM, *Journal of Geophysical
845 Research: Atmospheres*, 115(D14), D14121, doi:10.1029/2009JD013181.
- 846 Otto-Bliesner, B. L., E. C. Brady, J. Fasullo, A. Jahn, L. Landrum, S. Stevenson, N. Rosenbloom, A. Mai, and G. Strand
847 (2016), Climate Variability and Change since 850 CE: An Ensemble Approach with the Community Earth System
848 Model, *Bulletin of the American Meteorological Society*, 97(5), 735-754, doi:10.1175/bams-d-14-00233.1.
- 849 Potts, K. A. (2017), Poster: The South East Asian Aerosol Plume: The Cause of All El Niño Events, in *AGU 2017 Fall
850 Meeting*, edited, Earth and Space Science Open Archive (ESSOAr, New Orleans, USA,
851 doi:<https://doi.org/10.1002/essoar.10500075.1>).
- 852 Ralph, F. M., and M. D. Dettinger (2011), Storms, floods, and the science of atmospheric rivers, *Eos, Transactions
853 American Geophysical Union*, 92(32), 265-266, doi:10.1029/2011EO320001.
- 854 Ramanathan, V. (2006), ATMOSPHERIC BROWN CLOUDS: HEALTH, CLIMATE AND AGRICULTURE
855 IMPACTS, *Scripta Varia* 106.
- 856 Remer, L. A., et al. (2009), Executive Summary, in *Atmospheric Aerosol Properties and Climate Impacts, A Report by
857 the U.S. Climate Change Science Program and the Subcommittee on Global Change Research* [Mian Chin, Ralph A.
858 Kahn, and Stephen E. Schwartz (eds.)]. National Aeronautics and Space Administration, Washington, D.C., USA.
- 859 Remer, L. A., et al. (2005), The MODIS Aerosol Algorithm, Products, and Validation, *Journal of the Atmospheric
860 Sciences*, 62(4), 947-973, doi:10.1175/JAS3385.1.
- 861 Schaller, N., et al. (2016), Human influence on climate in the 2014 southern England winter floods and their impacts,
862 *Nature Clim. Change*, 6(6), 627-634, doi:10.1038/nclimate2927
863 <http://www.nature.com/nclimate/journal/v6/n6/abs/nclimate2927.html#supplementary-information>.
- 864 Seifkar, N., X. Lu, M. Withers, R. Malina, R. Field, S. Barrett, and H. Herzog (2015), Biomass to Liquid Fuels
865 PathwaysRep.
- 866 Solomon, S., et al. (2007), Technical Summary. In: *Climate Change 2007: The Physical Science Basis. Contribution of
867 Working Group I to the Fourth Assessment Report of the Intergovernmental Panel on Climate Change* [Solomon, S., D.
868 Qin, M. Manning, Z. Chen, M. Marquis, K.B. Averyt, M. Tignor and H.L. Miller (eds.)]. Cambridge University Press,
869 Cambridge, United Kingdom and New York, NY, USA.
- 870 Sterl, A., C. Severijns, H. Dijkstra, W. Hazeleger, G. Jan van Oldenborgh, M. van den Broeke, G. Burgers, B. van den
871 Hurk, P. Jan van Leeuwen, and P. van Velthoven (2008), When can we expect extremely high surface temperatures?,
872 *Geophysical Research Letters*, 35(14), doi:10.1029/2008gl034071.
- 873 van Oldenborgh, G. J., S. Drijfhout, A. van Ulden, R. Haarsma1, A. Sterl, C. Severijns, W. Hazeleger, and H. Dijkstra
874 (2009), Western Europe is warming much faster than expected, *Climate of the Past*, 5, 1 - 12.
- 875 Venzke, E. (2013), *Volcanoes of the World v. 4.4.3*, edited by S. I. G. V. Program, doi:
876 <http://dx.doi.org/10.5479/si.GVP.VOTW4-2013>.
- 877 Vicente-Serrano, S. M., and J. I. López-Moreno (2006), The influence of atmospheric circulation at different spatial
878 scales on winter drought variability through a semi-arid climatic gradient in Northeast Spain, *International Journal of
879 Climatology*, 26(11), 1427-1453, doi:10.1002/joc.1387.
- 880 Wang, C. (2004), A modeling study on the climate impacts of black carbon aerosols, *Journal of Geophysical Research:
881 Atmospheres*, 109(D3), D03106, doi:10.1029/2003JD004084.
- 882 Winker, D. M., M. A. Vaughan, A. Omar, Y. Hu, K. A. Powell, Z. Liu, W. H. Hunt, and S. A. Young (2009), Overview
883 of the CALIPSO Mission and CALIOP Data Processing Algorithms, *Journal of Atmospheric and Oceanic Technology*,
884 26(11), 2310-2323, doi:10.1175/2009jtecha1281.1.
- 885 Yiou, P., R. Vautard, P. Naveau, and C. Cassou (2007), Inconsistency between atmospheric dynamics and temperatures
886 during the exceptional 2006/2007 fall/winter and recent warming in Europe, *Geophysical Research Letters*, 34(21),
887 L21808, doi:10.1029/2007GL031981.

888 Young, A. M., K. T. Skelly, and J. M. Cordeira (2017), High-impact hydrologic events and atmospheric rivers in
889 California: An investigation using the NCEI Storm Events Database, *Geophysical Research Letters*, *44*(7), 3393-3401,
890 doi:10.1002/2017GL073077.
891 Zhang, R., et al. (2013), Have Aerosols Caused the Observed Atlantic Multidecadal Variability?, *Journal of the*
892 *Atmospheric Sciences*, *70*(4), 1135-1144, doi:doi:10.1175/JAS-D-12-0331.1.
893